Water restrictions under climate change: a Rhone-Mediterranean perspective combining 'bottom up' and 'top-down' approaches

Eric SAUQUET[1], Bastien RICHARD[1,2], Alexandre DEVERS[1], Christel PRUDHOMME[3,4,5]

Correspondance to : E. Sauquet (eric.sauquet@irstea.fr)

[1] Irstea, UR Riverly, 5 rue de la Doua CS20244, 69625 Villeurbanne cedex, France

[2] Irstea, UMR G-EAU, Water resource management, Actors and Uses Joint Research Unit, Campus Agropolis - 361 rue Jean-François Breton – BP 5095, 34196 Montpellier Cedex 5, France

[3] European Centre for Medium-Range Weather Forecasts, Reading, UK

[4] Department of Geography, Loughborough University, Loughborough, LE11 3TU, UK

[5] NERC Centre for Ecology & Hydrology, Maclean Building, Benson Lane, Crowmarsh Gifford, Wallingford, Oxon, OX10 8BB, UK

Abstract Drought management plans (DMPs) require an overview of future climate conditions for ensuring long term relevance of existing decision-making processes. To that end, impact studies are expected to best reproduce decision-making needs linked with catchment intrinsic sensitivity to climate change. The objective of this study is to apply a risk-based approach through sensitivity, exposure and performance assessments to identify where and when, due to climate change, access to surface water constrained by legally-binding water restrictions may question agricultural activities. After inspection of legally-binding water restrictions (WR) from the DMPs in the Rhône-Méditerranée (RM) district, a framework to derive WR durations was developed based on harmonized low-flow indicators. Whilst the framework could not perfectly reproduce all WR ordered by state services, as deviations from socio-political factors could not be included, it enabled to identify most WRs under current baseline, and to quantify the sensitivity of WR duration to a wide range of perturbed climates for 106 catchments. Four classes of responses were found across the RM district. The information provided by the national system of compensation to farmers during the 2011 drought was used to define a critical threshold of acceptable WR, related to the current activities over the RM district. The study finally concluded that catchments in mountainous areas, highly sensitive to temperature changes, are also the most predisposed to future restrictions under projected climate changes considering current DMPs, whilst catchments around the Mediterranean Sea, were found mainly sensitive to precipitation changes and irrigation use was less vulnerable

to projected climatic changes. The tools developed enable a rapid assessment of the effectiveness of current DMPs under climate change, and can be used to prioritize review of the plans for those most vulnerable basins.

Keywords Climate change; drought management plan; low-flow; France; scenario-neutral approach; response surface; vulnerability; water restriction.

1 Introduction

The Mediterranean region is known as one of the "hot spots" of global change (Giorgi 2006; Paeth *et al*. 2017) where environmental and socio-economic impacts of climate change and human activities are likely to be very pronounced. The intensity of the changes is still uncertain, however, climate models agree on significant future increase in frequency and intensity of meteorological, agricultural and hydrological droughts in Southern Europe (Jiménez Cisneros *et al.* 2014; Touma *et al*. 2015), with climate change likely to exacerbate the variability of climate with regional feedbacks affecting Mediterranean-climate catchments (Kondolf *et al.* 2013). Facing more severe low-flows and significant losses of snowpack, southeastern France will be subject to substantial alterations of water availability: Chauveau *et al.* (2013) have shown a potential increase in low-flow severity by the 2050's with a decrease in low-flow statistics to 50% for the Rhône River near its outlet. Andrew and Sauquet (2017) have reported that global change will most likely result in a decrease in water resources and an increase both in pressure on water resources and in occurrence of periods of water limitation within the Durance River basin, one of the major water tower of Southeastern France. In addition Sauquet *et al.* (2016) have suggested the need to open the debate on a new future balance between the competing water uses. More recently, based on climate projections obtained from Coupled Model Intercomparison Project Phase 5 (Taylor *et al*. 2012), Dayon *et al*. (2018) have shown a significant increase in hydrological drought severity with a meridional gradient (up to -55% in southern France for both the annual minimum monthly flow with a return period of 5 years and the mean summer river flow) while a more uniform increase in agricultural drought severity is projected over France for the end of the 21st century.

The challenges associated with possible impact of climate change on droughts have received increasing attention by researchers, stakeholders and policy makers in the last decades. To date climate change impact studies are usually dedicated to water resources (*e.g*., Vidal *et al.* 2016, Collet *et al.* 2018, Hellwig and Stahl 2018, Samaniego *et al.* 2018) or water needs for the competing users (*e.g*., Bisselink *et al*., 2018). However, examining the suitability of regulatory instruments, such as Drought Management Plans, is also essential to

establish successful adaptation strategies. These plans state which type of water restrictions should be imposed to non-priority uses during severe low-flow events; under climate change, those water restrictions and stakeholders' access to water resources might need to be revised as drought patterns and severity might change. In most climate change impact studies, analyses on the regulatory measures are often limited to maintaining environmental flows – especially when assessing future hydropower potential. To date, no climate change impact on water regulatory measures have yet been assessed at the regional scale, highlighting a gap in developing robust adaptation plans. This study aims to address this gap by suggesting a framework, applying it to southeastern France and publishing the associated results..

The paper develops a framework to simulate legally-binding water restrictions (WR) under climate change in the Rhone-Méditerranée district (southeastern France) and to assess the likelihood of future restrictions depending on their sensitivity, performance and exposure to climate deviations. The approach is adapted from the risk-based approaches such as developed in parallel by Brown *et al*. (2011) − named "Decision Tree Framework" − and Prudhomme *et al*. (2010) − named "Scenario neutral approach"− and aims to establish a ranking of areas in terms of vulnerability to climate change in terms of access to water for agricultural uses. This research is a scientific contribution to the ongoing decade 2013–2022 entitled "Panta Rhei – Everything Flows" initiated by the International Association of Hydrological Sciences and more specifically to the "Drought in the Anthropocene" working group (https://iahs.info/Commissions--W-Groups/Working-Groups/Panta-Rhei/Working-Groups/Drought-in-the-Anthropocene.do, Van Loon *et al*. 2016). Legally-binding water restrictions and their associated decision-making processes are important for the blue water footprint assessment at the catchment scale.

The paper is organized in four parts. Sect. 2 introduces the area of interest and the source of data. Sect. 3 is a synthesis of the mandatory processes for managing drought condition implemented within the Rhône-Méditerranée district and the related water restriction orders adopted over the period 2005-2016. Sect. 4 describes the general modelling framework developed to simulate WR decisions. The approach is implemented at both local and regional scales and results discussed in Sect. 5 before drawing general conclusions in Sect. 6.

2 Study area and materials

2.1 Study area

The Rhone-Méditerranée district covers all the Mediterranean coastal rivers and the French part of the Rhône River basin, from the outlet of Lake Geneva to its mouth (Fig. 1). Climate is rather varied with a temperate influence in the north, a continental influence in the mountainous areas and a Mediterranean climate with dry and hot summers dominating in the south and along the coast. In the mountainous part (in both the Alps and the Pyrenees) the snowmelt-fed regimes are observed in contrast to the northern part under oceanic climate influences, where seasonal variations of evaporation and precipitation drive the monthly runoff pattern (Sauquet *et al.* 2008).

Water is globally abundant but unevenly between the mountainous areas, the northern and southern parts of the Rhône-Méditerranée (RM) district and water resources are under high pressure due to water abstractions. For the period 2008-2013, annual total water withdrawal was around 6 billion of m^3 in the (excluding any water abstraction for energy such as cooling nuclear plants and hydropower) with a more than used for irrigation (3.4 billion of m^3, including 2 billion of m^3 for channel conveyance). Use for public and industrial supply is of 1.6 and 1 billion of m^3, respectively. Because of an intense competition for water between different users — agricultural, municipal, and industrial — and the environment, some areas within the RM district can be vulnerable during low-flow periods. Around 40% of the RM district sufferis from water stress and scarcity (http://www.rhone-mediterranee.eaufrance.fr/gestion/gestion-quanti/problematique.php) and has been identified by the French RM Water Agency as areas with persistent imbalance between water supply and water demand.

2.2 Drought management plan

Drought management plans (DMPs) define specific actions to be undertaken to enhance preparedness and increase resilience to drought. In France DMPs include regulatory frameworks to be applied in case of drought, named "arrêtés cadres sécheresse". The past and operating DMPs and the water restriction orders were inspected in the 28 departments of the RM district. They were obtained from:

- The database of the *DREAL Auvergne-Rhône-Alpes ("Direction Régionale de l'Eau, de l'Alimentation et du Logement" in French)* including WR levels and duration at the catchment scale available over the period 2005-2016 within the RM district;

- The online national database PROPLUVIA (http://propluvia.developpement-durable.gouv.fr) with WR levels and dates of adoption at the catchment scale for the whole France available from 2012.

The most recent consulted documents date from January 2017.

2.3 Hydrological data

The hydrological observation dataset is a subset of the 632 French near-natural catchments identified by Caillouet *et al.* (2017). Daily flow data from 1958 to 2013 were extracted from the French HYDRO database (http://hydro.eaufrance.fr/). Time series with more than 30% of missing values or more than 30% of null values were disregarded. Finally the total dataset consist of 106 gauged catchments located in the RM district with minor human influence and with high quality data. The selected catchments are benchmark catchments where near natural drought events are observed and current water availability is monitored. Water can be abstracted from other nearby streams.

A selection of 15 evaluation catchments (Table 1) were used to calibrate and to evaluate the Water Restriction Level modelling framework (Sect. 4), selected because (*i*) they have complete records of stated water restriction, including dates and levels of restrictions - which was not the case of other catchments, and (*ii*) they are located in areas where water restriction decisions are frequent. To facilitate interpretation, the 15 catchments have been ordered along the north-south gradient. The Ouche and Argens River basins (n°1 and 15 in Table 1) are the northernmost and the southernmost gauged basins, respectively. The 15 catchments encompass a large variety of river flow regimes according to the classification suggested by Sauquet *et al.* (2008) (see Appendix A) that can be observed in the RM district (*e.g.*, the Ouche (1 in Table 1, pluvial regime), Roizonne (3, transition regime) and Argens (15, snowmelt-fed regime) River basins).

2.4 Climate data

Baseline climate data were obtained from the French near-surface Safran meteorological reanalysis (Quintana-Seguí *et al.*, 2008; Vidal *et al.* 2010) onto an 8-km resolution grid from 1 August 1958 to 2013. Exposure data was based on the regional projections for France (Table 2) available from the DRIAS French portal (www.drias-climat.fr, Lémond *et al*. 2011). Catchment-scale data were computed as weighted mean for temperature and sum for precipitation based on the river network elaborated by Sauquet (2006).

3 Operating Drought Management Plans in the Rhône-Méditerranée district

The French Water Act amended on September 24, 1992 (decree n°92/1041) defines the operating procedures for the implementation of drought management plan (DMP). Following the 2003 European heat wave, drought management plans including water restrictions have been gradually implemented in France (MEDDE 2004). Water restrictions fall within the responsibility of the prefecture (one per administrative unit or department), as mentioned in article L211-3 II-1° of the French environmental code. Their role in drought management is to ensure that regulatory approvals for water abstraction continuously meet the adequate balance between water resource availability and water uses or ecosystems resilience. *De facto*, legally-binding water restrictions have to fulfill three principles: (*i*) being gradually implemented at the catchment scale in regard with low-flow severity observed at various reference locations, (*ii*) ensuring users equity and upstream-downstream solidarity and (*iii*) being time-limited to fix cyclical deficits rather than structural deficits. The prefecture is in charge of establishing and monitoring the DMP operating in the related department.

Past and current drought management plans were analyzed to identify the past and current modalities of application, the frequency of water restriction orders and the areas affected by water restrictions. Gathering and studying the regulatory documents was a tedious in particular because of their lack of clear definition of the hydrological variables used in the decision-making process.

This analysis shows that the implementation of the DMPs has evolved for many departments since 2003, *e.g.*, with changes in the terminology and a national scale effort to standardize WR levels. Now severity in low-flows is classified into four levels which are related to incentive or legally-binding water restrictions. These measures affect recreational uses, vehicle washing, lawn watering and domestic, irrigation and industrial uses (Table 3). Level 0 (named “vigilance”) refers to incentive measures, such as awareness campaign to promote low water consumption from public bodies and general public. Levels 1 to 3 are incrementally legally-binding restriction levels; level 1 (named “alert”) and 2 (named “reinforced alert”) enforcing reductions in water abstraction for agriculture uses, or several days a week of suspension; level 3 (named “crisis”) involves a total suspension of water abstraction for non-priority uses, including abstraction for agricultural uses and home gardening, and authorizes only water abstraction for drinking water and sanitation services. Due to change in the naming of WR levels since their creation one task was dedicated to restate the WR decisions (hereafter “OBS”) since 2005 with respect to the current classification into four WR levels.

For all catchments, a WR decision chronology was derived, showing a large spatial variability in WR (Fig. 1) - note that the 15 evaluation catchments (Table 1) are located in the most affected areas. Between 2005 and 2012, WR decisions were mainly adopted between April and October (98% of the WR decisions, Fig. 2), with 62% in July or August, peaking in July.

Decisions for adopting, revoking or upgrading a WR measure are taken after consultation of "drought committees" bringing the main local stakeholders together, the meeting frequency of which is irregular and depends on hydrological drought development. The adopted restriction level is mainly based on the existing hydrological conditions at the time, i.e., based on low-flow monitoring indicators measured at a set of reference gauging stations and their departure from a set of regulatory thresholds. This varies greatly across the RM district (Fig. 3). The low-flow monitoring indicators usually considered are:

- the daily discharge *Qdaily*,
- the *d*-day maximum discharge *QCd*, $QCd(t)=\max\left(Qdaily(t'),t'\in\left[t-d+1,t\right]\right)$ and
- the *d*-day mean discharge *VCd*, $VCd(t)=\int_{t-d+1}^{t} Qdaily(t')\,dt'$

with duration *d* associated with WR decision varying between 2 and 10 days depending on DMPs. *VC*3 (40% of DMPs) and *QC*7 (17% of DMPs) are the most commonly used, but other single indicators include *Qdaily* (17%), *QC*5 (14%), *QC*10 (8%), *QC*2 (3%), *VC*10 (3%), and with mixed indicators also used (*e.g.*, 14% of *VC*3 and *Qdaily* together.

The threshold associated with WR also varies within the district, generally associated with statistics derived from low-flow frequency analysis, but also fixed to locally-defined ecological requirements. In the context of DMPs, series of minimum *QCd* or *VCd* are calculated by the block minima approach and thereafter fitted to a statistical distribution. The block is not the year but the month or given by the division of the year into 37 10-day time-window. The regulatory thresholds are given by quantiles with four different recurrence intervals associated to the four restriction levels. Generally, return periods *T* of 2, 5, 10 and 20 years are associated with the "vigilance", "alert", "reinforced alert" and "crisis" restriction levels, respectively. For example, let us consider thresholds based on the annual monthly minima of *VCNd*. The block minima approach is carried out on the *N* years of records for each month *i*, $i=1\ldots,12$ leading to twelves datasets $\{min\{VCNd(t), month(t)=i, year(t)=j\}, j=1,\ldots,N\}$. The twelve fitted distribution allows the calculation of 48 values of thresholds (=12 months × 4 levels) with four *T*-year recurrence intervals.

The meteorological situation is also examined in terms of precipitation deficit and likelihood of significant rainfall event considering available short to medium-range weather forecasts. There are heterogeneities in the drought monitoring variables, the time period on which deficit is calculated and the permissible deviation from long term average values.

Where appropriate other supporting local observations such as groundwater levels, reservoir water levels, field surveys provided by the ONDE network (Beaufort *et al*., 2018) or feedbacks from stakeholders can be used to inform final decisions.

4 Risk-based framework and the related tools

4.1 The scenario neutral concept

Traditionally, hydrological impact studies are often based on "top down" (scenario-driven) approaches, easy to interpret, but with associated conclusions becoming outdated as new climate projections are produced. In addition scenario-based studies may fail to match decision-making needs since the implication in terms of water management is usually ignored (Mastrandrea *et al.* 2010). As a substitute to scenario-driven approach, the scenario-neutral approach (Brekke *et al*. 2009, Prudhomme *et al*. 2010, 2013a, 2013b, 2015, Brown *et al*. 2012, Brown and Wilby 2012, Culley *et al*. 2016, Danner *et al*. 2017) has been developed to better address risk-based decision issues. The suggested framework shifts the focus on the current vulnerability of the system affected by changes and on critical thresholds above which the system starts to fail to identify possible maladaptation strategies (Broderick *et al*. 2019). Applied to water management issues, the scenario-neutral studies (*e.g.*, Weiß 2011, Wetterhall *et al.* 2011, Brown *et al.* 2011, Whateley *et al.* 2014) aim at improving the knowledge of the system's vulnerability to changes and at bridging the gap between scientists and stakeholders facing needs in relevant adaptation strategy. Prudhomme *et al*. (2010) have suggested combining of the sensitivity framework with 'top-down' projections through climate response surfaces. This approach has been applied to low-flows in the UK (Prudhomme *et al*. 2015) and its interests have been discussed as a support tool for drought management decisions.

The risk-based framework adopted contains three independent components (Fig. 4):

(i) Sensitivity analysis (Fronzek *et al*., 2010) based on simulations under a large spectrum of perturbed climates to (a) quantify how policy-relevant variables respond to changes in different climate factors, and (b) identify the climate factors to which the system is the most sensitive. Addressing (a) and (b)

may help modelers to check the relevance of their model (*e.g.*, unexpected sensitivity to a climate factor regarding the know processes influencing the rainfall-runoff transformation). From an operational viewpoint, it may encourage stakeholders to monitor in priority the variables that affect the system of interest (reinforcement of the observation network, literature monitoring, etc.),

(ii) Sustainability or performance assessment, aiming to identify under which climate (or others) conditions (e.g., no rain period in spring, heat wave in summer, etc.) the system fails. A key-challenge in bottom-up framework is to define performance metrics and associated critical thresholds relevant for the system of interest. In the case of our study, this would be acceptable or not water restrictions for users,

(iii) Exposure, as defined by state-of-the-art regional climate trajectories superimposed to the climate response surface The exposure measures the probability of changes occurring for different lead times based on available regional projections..

All the components of the framework together contribute to the vulnerability of the system (including its management) to systematic climatic deviations.

The sensitivity analysis was conducted applying a water restriction modelling framework. Climate conditions were generated applying incremental changes to historical data (precipitation and temperature) and introduced as inputs in the developed models to derive occurrence and severity of water restriction under modified climates. The tool chosen here to display the interactions between water restriction and the parameters that reflect the climate changes is a two-dimensional response surface, with axes represented by the main climate drivers. This representation is commonly used in scenario neutral approach. For example, in both Culley *et al*. (2016) and Brown *et al*. (2012) the two axes were defined by the changes in annual precipitation and temperature. When changes affect numerous attributes of the climate inputs, additional analyses (*e.g.*, elasticity concept combined with regression analysis (Prudhomme *et al*. 2015), Spearman rank correlation and Sobol' sensitivity analyses (Guo *et al*. 2017)) may be required to point out the key variables with the largest influence on water restriction that form thereafter the most appropriate axes for the response surfaces.

Performance assessment is a challenging task for hydrologists since it requires information on the impact of extreme hydrometeorological past events on stakeholders' activities. Simonovic (2010) used observed past events selected with local authorities on a case study in southwestern Ontario (Canada), chosen for their past impact (flood peak associated with a top-up of the embankments of the main urban center; level II drought

conditions of the low water response plan). Schlef *et al*. (2018) set the threshold to the worst modelled event under current conditions. Whateley *et al.* (2014) assessed the robustness of a water supply system and the threshold is fixed to the cumulative cost penalties due to water shortage evaluated under the current conditions. Brown *et al*. (2012) and Ghile *et al*. (2014) suggested selecting thresholds according to expert-judgment of unsatisfactory performance of the system by stakeholders, whilst Ray and Brown (2015) use results from benefit-cost analyses. The spatial coverage of a large area, such as the RM district, and the heterogeneity in water use (domestic needs, hydropower, recreation, irrigation, etc.) makes it challenging for a systematic, consistent and comparable stakeholder consultation to be conducted and for a relevant critical threshold T_c to be fixed for all the users. Facing this complexity, only the irrigation water use will been examined here, since it is the sector which consumes most water at the regional scale, with a critical threshold defined for this single water use.

Exposure to changes here is measured using regional projections, visualized graphically by positioning the regional projections in the coordinate system of the climate response surfaces and identifying the associated likelihood of failure relative to T_c. Note that, to update the risk assessment, only the exposure component has to be examined (including the latest climate projections available onto the response surfaces).

4.2 The rainfall-runoff modelling

The conceptual lumped rainfall-runoff model GR6J was adopted for simulating daily discharge at 106 selected catchments of the RM district. The GR6J model is a modified version of GR4J originally developed by Perrin *et al.* (2003), well suited to simulate low-flow conditions (Pushpalatha *et al.* 2011). It was selected for its good performance across a large spectrum of river flow regimes (*e.g*., Hublart *et al.* 2016, Poncelet *et al*. 2017).

The GR6J model has six parameters to be fitted (Fig. 5): the capacity of soil moisture reservoir (X1) and of the routing reservoir (X3), the time base of a unit hydrograph (X4), two parameters of the groundwater exchange function F (X2 and X5) and a coefficient for emptying exponential store (X6). The GR6J model is combined here with the CemaNeige semi-distributed snowmelt runoff component (Valéry *et al*. 2014). The catchment is divided into five altitudinal bands of equal area on which snowmelt and snow accumulation processes are represented. For each band, daily meteorological inputs – including solid fractions of precipitation - are extrapolated using elevation as covariate and the snow routine is calculated separately. Finally, its outputs are then aggregated at the catchment scale to feed GR6J. The two parameters of Cemaneige are: the parameter

controlling snowpack inertia (X1) and the degree-day coefficient controlling snowmelt (X2). No routine to simulate water management (*e.g.*, reservoir) was considered here since discharges of the 106 gauging stations are weakly altered by human actions or naturalized discharges. The eight parameters (six from the GR6J model and two from the CemaNeige module) were calibrated against the observed discharges using the baseline Safran reanalysis as input data and the Kling–Gupta efficiency criterion (Gupta *et al*. 2009) KGE_{SQRT} calculated on the square root of the daily discharges as objective function. The KGE_{SQRT} criterion was used to give less emphasis of extreme flows (both low and high flows). As the climate sensitivity space includes unprecedented climate conditions (including colder climate conditions around the current-day condition), the CemaNeige module was run for all the 106 catchments even for those not currently influenced by snow.

The two step procedure suggested by Caillouet *et al.* (2017) was adopted for the calibration: first the eight free parameters were fitted only for the catchments significantly influenced by snowmelt processes – *i.e.*, when the proportion of snowfall to total precipitation > 10% - and second, for the other catchments, the medians of the CemaNeige parameters were fixed and the six remaining parameters are then calibrated. Calibration is carried out over the period 1 January 1973 to 30 September 2006 with a 3-year spin-up period to limit the influence of reservoir initialization on the calibration results. The criterion KGE_{SQRT} and the Nash-Sutcliffe efficiency criterion on the log transformed discharge NSE_{LOG} (Nash and Sutcliffe 1970) were calculated over the whole period 1958-2013 for the subset of 15 evaluation catchments (Table 1), showing KGE_{SQRT} and NSE_{LOG} values are above 0.80 and 0.70 respectively. These two goodness-of-fit statistics indicate that GR6J adequately reproduces observed river flow regime, from low to high flow conditions. The less satisfactory performances of GR6J are observed for the Tarn and Roizonne River basins, both characterized by smallest drainage areas and highest elevations of the dataset. These lowest performances are likely to be linked to their location in mountainous areas (snowmelt processes are difficult to reproduce) and to their size (the grid resolution of the baseline climatology fails to capture the climate variability in the headwaters).

4.3 The water restriction level modelling framework

The Water Restriction Level (WRL) modelling framework developed aims to identify periods when the hydrological monitoring indicator is consistent with legally-binding water restrictions. Only physical components (mainly hydrological drought severity) leading to WR decisions are considered, with no socio-political factor accounted for to model water restrictions.

To enable comparison of results across all catchments, the same drought monitoring indicators and regulatory thresholds were adopted in all the catchments (see Section 3 for details), selected as most commonly used in the 28 DMPs across the RM district, specifically *VC*3 as monitoring indicator and 10*d*-*VCN*3 with return periods *T* of 2, 5, 10 and 20 years as regulatory thresholds. Each regulatory threshold is defined for a 10-day calendar period between 1st April and 31st October, resulting in 21 sets of four thresholds. Water restrictions are decided after consulting drought committees that convene irregularly depending on hydrological conditions over a time window, i.e. the last *N* days. Here a time window for analysis of *N*= 10 days was decided, which is consistent with the prefectural decision-making time frame (frequency of updates in water restriction statements). The WRL modelling time-step is finally fixed to 10 days and a representative value of WRL is given to the 21 10-day calendar periods from April to October. Thus WRL is thus computed as follows:

- *VC*3(*t*) is computed from daily discharge *Qdaily*(*t*) every day *t*;
- *VC*3(*t*) is compared to the corresponding regulatory thresholds to create time series of daily water restriction level *wrl*, with *wrl*(*t*) ranging from 0 ('no alert') to 3 ('crisis'):
    - if 10*d*-*VCN*3(2) ≥ *VC*3(*t*) > 10*d*-*VCN*3(5), *wrl*(*t*)=0
    - if 10*d*-*VCN*3(5) ≥ *VC*3(*t*) > 10*d*-*VCN*3(10), *wrl*(*t*)=1
    - if 10*d*-*VCN*3(10) ≥ *VC*3(*t*) > 10*d*-*VCN*3(20), *wrl*(*t*)=2
    - if 10*d*-*VCN*3(20) ≥ *VC*3(*t*), *wrl*(*t*)=3
- A dekad *WRL(d)* time series is created as the median of *wrl*(*t*) for each 10-day period;
- The *WRL*(*d*) value is set to zero if preceding 10-day precipitation total exceeds 70% of inter-annual precipitation average(precipitation correction).

Inputs of the WRL model are daily discharges and precipitation. Outputs are WRL dekad time series. Modelling is only applied to the period April-to-October, the irrigation period and when most water restrictions are put in place. The low-flow monitoring indicator *VC*3 and the regulatory thresholds 10*d*-*VCN*3(*T*) are computed from daily discharge time series *Qdaily* based on full period of records prior to 31st December 2013. The log-normal distribution is used to assess the return periods.

The WRL modelling framework is can be applied to both observed and simulated time series. For the later, outputs from GR6J are used for simulations under current and modified climate conditions. Regulatory thresholds are derived from simulated discharge using the Safran baseline meteorological reanalysis as input, to moderate the possible effect of bias in rainfall-runoff modelling.

The WRL modelling framework was verified in the 15 evaluation catchments (Table 1). WRL simulations based on modelled (hereafter "GR6J") and observed (hereafter 'HYDRO') discharge were compared graphically to official WR measures ("OBS") . A further assessment was conducted using the *Sensitivity* and *Specificity* scores (Jolliffe and Stephenson, 2003) to examine how well the WRL modelling framework can discriminate WR severity levels (Table 4). The *Sensitivity* score assesses the probability of event detection; the *Specificity* score calculates the proportion of "No" events that are correctly identified. An event was defined as any legally-binding Water Restriction of at least level 1, and 'non-event' a period where WRL is 0 or without WR. Comparisons were made over the 2005-2013 period, corresponding to the common period of availability for OBS, HYDRO and GR6J.

Fig. 6 shows years with severe simulated WRLs (*e.g.*, 2005 and 2011) and years with no or few simulated WRs (*e.g.*, 2010 and 2013). Both GR6J and HYDRO simulations are generally consistent with OBS, even if misses are found (*e.g.*, basins 9 to 11 during the year 2005). There is no systematic bias, with some overestimations (e.g., 2005 using GR6J in basins 1 and 15; 2007 using HYDRO in basin 15), underestimations (e.g. 2009 in basin 6, 7, and 8) and misses (e.g. 2005 using HYDRO in basin 1).

Sensitivity and *Specificity* scores computed with OBS considered as benchmark (Fig. 7) show a large variation across the catchments, in particular for *Sensitivity*. *Specificity* scores are around 0.85 for both GR6J and HYDRO, suggesting that more than 85% of the observed non-events were correctly simulated by the WRL modelling framework. The median of WRL *Sensitivity* score using HYDRO is around 45%, indicating that for half the catchments, less than 45% of observed events are detected based on HYDRO discharges, but this raises to 68% of events detected when WRLs are simulated based on GR6J discharge. No evidence of systematic bias associated with catchment location or river flow regime was found: northern (blue) and southern (red) catchments are uniformly distributed in the *Sensitivity*/*Specificity* space.

Sensitivity and *Specificity* scores using HYDRO as benchmark in the contingency table were also used to compare simulations from GR6J discharge with those obtained from HYDRO discharge. Median values reach 84% (*Sensitivity*) and 92% (*Specificity*), showing high consistency between HYDRO and GR6J. No statistical link between hydrological model and WRL model performance was found, with R^2 between NSE_{LOG} and *Sensitivity*, or NSE_{LOG} and *Specificity* lower than 7%. In addition, the similar skill scores of GR6J and HYDRO modelling suggest that possible biases in rainfall-runoff modelling does not impact on the ability of the WRL modelling framework to correctly simulate declared or not declared WRs. No evidence was found that the

slightly higher *Sensitivity* scores for GR6J was due to a "smoothing" introduced by the hydrological modelling (similar autocorrelation between observed and GR6J simulated *VC*3 time series VC3), but the relatively short verification period (only three years with legally-binding water restrictions in some catchments) and the frequency of DMP updates (black vertical segments in Fig. 6) might result in not truly representative scores.

Discrepancy between simulated and adopted WR measures is most likely due to the other factors involved in the making-decision process. When regulatory thresholds are crossed, restrictive measures should follow the DMPs. In reality, the measures are not automatically imposed, but are the result of a negotiating process. This process includes for example some expert-judgment factors such as (i) the evolution of low-flow monitoring indicators and thresholds over the years (*e.g.*, annual revision for the Ouche, and irregular revision for the Isère (38), Gard (30), Alpes-de-Haute-Provence (04) and Lozère (48) departments (last one in 2012); (ii) the role of drought committees in negotiating a delay in WR level applications to limit economic damages or to harmonize responses across different administrative sectors sharing the same water intake; (iii) the local expertise especially regarding the uncertainty in flow measurements (Barbier *et al*. 2007) impacting on the low-flow monitoring indicators, *e.g.*, Cote d'Or (21) and Lozère (48) in the northern and southwestern parts of the RM district, respectively. Note that where WR decisions are not uniquely based on hydrological indicators but also involve a negotiation process, the results of the WRL modelling framework should be interpreted as potential hydrological conditions for stating water restrictions.

Results of our sample study on 15 evaluation catchments show deviations for most catchments, but links between order restrictions and hydrological drought severity. These deviations may partly be attributed to the use of the same monitoring indicator and regulatory thresholds across the catchments in the modelling (whilst it is not true in reality), as a necessary assumption for a region scale analysis. Tests with *QC*7 as low-flow monitoring variable combined with the two dominant modalities for the regulatory thresholds show a weak sensitivity of the WRL modelling skill to the choice of the indicators (with a slight increase in *Specificity* score (~ 90%) while *Sensitivity* score is reduced (< 50%) using GR6J). Whilst the developed WRL modelling framework does not account for expert-decision brought by drought committees - and hence is not designed to simulate the exact WR decisions - its ability to simulate 68% of the stated restrictions over the period 2005-2013 demonstrates its usefulness as a tool to objectively simulate the potential of drought restrictions based on hydrological drought physical processes. The methodology was applied to the 106 catchments of the RM district under climate

perturbations to assess the potential impact of climate change on water restriction in the region. The resulting analysis focuses on water restriction level higher than 1, denoted thereafter WR*.

4.4 The generation of perturbed climate conditions

The generation of climate response surfaces relies on synthetic climate time series representative of each explore climate condition, and used as input to the impact modelling chain (here hydrological model and WRL modelling framework). Methods based on stochastic weather simulation have been used (*e.g.*, Steinschneider and Brown 2013, Cipriani *et al*. 2014, Guo *et al*. 2016, 2017), but they can be complex to apply in a region with such heterogeneous climate as the RM district. Alternatively, the simple "delta-change" method (Arnell 2003) has been commonly used to provide a set of perturbed climates in scenario-neutral approach (*e.g.*, Paton *et al*. 2013, Singh *et al*. 2014), and was used here, similarly to (Prudhomme *et al*. 2010, 2013a, 2013b, 2015).

Following Prudhomme *et al*. (2015), monthly correction factors ΔP and ΔT are calculated using single-phase harmonic functions:

$$\Delta \mathrm{P}(i) = \mathrm{P}_0 + \mathrm{Ap} \cdot \cos\left[(i - \varphi_{\mathrm{P}}) \cdot \frac{\pi}{6}\right]. \quad (1)$$

$$\Delta \mathrm{T}(i) = \mathrm{T}_0 + \mathrm{A}_{\mathrm{T}} \cdot \cos\left[(i - \varphi_{\mathrm{T}}) \cdot \frac{\pi}{6}\right]. \quad (2)$$

with P_0 and T_0 + A_T mean annual changes in precipitation (1) and temperature (2), respectively; i indicator of the month (from 1 to 12); φ_P the phase parameter and A_p the semi-amplitude of change (*e.g.*, half the difference between highest and lowest values). These corrections factors were applied to the baseline climate data sets to create perturbed daily forcings:

$$\mathrm{P}^*(d) = \mathrm{P}(d) \cdot [\overline{\mathrm{PM}}(\mathrm{month}(d)) + \Delta \mathrm{P}(\mathrm{month}(d)]/\overline{\mathrm{PM}}(\mathrm{month}(d)) \quad (3)$$

$$\mathrm{T}^*(d) = \mathrm{T}(d) + \Delta \mathrm{T}\big(\mathrm{month}(d)\big) \quad (4)$$

with $P(d)$ and $T(d)$ baseline precipitation and temperature values for day d; $P^*(d)$ and $T^*(d)$ the corrected (or perturbed) values for day d;. $\overline{PM}(\mathrm{month}(d))$ average monthly baseline precipitation for month(d). Corrected potential evapotranspiration *PET**time series were derived from temperature values using the formula suggested by Oudin *et al* (2005):

$$\mathrm{PET}^*(d) = \max\left[\mathrm{PET}(d) + \frac{Ra}{28.5}\frac{\Delta T(\mathrm{month}(d))}{100}; 0\right]. \quad (5)$$

with PET(d) baseline potential evapotranspiration values for day d; Ra extra-terrestrial global radiation for the catchment.

The baseline climate (precipitation and temperature) time series were extracted from the Safran reanalysis over the period 1958-2013 (56 years), and perturbed time series generated for the same length. The range of climate change factors to generate the perturbed series were chosen to encompass both the range and the seasonality of RCM-based changes. on projections in France. A set of 45 precipitation and 30 temperature scenarios was created (Fig. 8), spanning the range of potential future climate suggested by Terray and Boé (2013) and combined independently, resulting in a total of 1350 precipitation and temperature perturbations pairs used to define the climate sensitivity space. In this application,

- P_0, (mm.an^{-1})= -20 +20/3× (j-1) , j= 1,.., 9 ,
- Ap (mm.season^{-1}) = 20/3× (j-1) , j= 1,.., 5 ,
- T_0 (°C.an^{-1}) = j-1 , j= 1,…, 6 ,
- A_T (°C.season^{-1}) = -0.5 +2×(j-1) , j= 1,…,5 ,
- φ_P parameter is fixed to 1 to consider minimum change in January and maximum change in July and
- φ_T is fixed to 2 to get maximum change in August.

5 Drought management plans under climate change and their impact on irrigation use

5.1 The Water Restriction response surfaces

The 1350 sets of perturbed precipitation, temperature and PET time series were each fed into the WRL modelling framework for each 106 catchments**.** Both *VC*3 (monitoring indicators) and 10*d*-*VCN*3(*T*) (regulatory thresholds) were computed from GR6J 56 years discharge simulations. For each scenario, the number of 10-day periods under Water Restriction of at least level 1 (WR*) were calculated, and expressed as deviation from the simulated baseline value: ΔWR*, hence removing the effect of any systematic bias from the WRL modelling framework. Results are shown as WR response surfaces built with *x*- and *y*-axes representing key climate drivers. Because different climate perturbation combinations share the same values of the key climate drivers, hence represented at the same location of the response surface, the median ΔWR* from all relevant combinations is displayed as color gradient, with the standard deviation *Sd* of ΔWR* showed as size of the symbol.

Response surfaces based on different climate variables for *x* (precipitation) and *y* (temperature) were generated over full or part of the water restriction period (April to October “AMJJASO”, March to June “MAMJ”; and July

443 to October "JASO", the latter coinciding with the highest temperatures) and visually inspected to identify the
444 greatest signal pattern, combined with the smallest dispersion around the surface response (i.e., analysis of the
445 median and the maximum of *Sd* values over the grid cells).

446 The response surfaces are exemplified on three of the 15 evaluation catchments (Table 1, Fig. 9):

447 - The Argens River basin, along the Mediterranean coast, severe low-flows occur in summer and actual
448 evapotranspiration is limited by water availability in the soil,
449 - The Ouche River basin, in the northern part of the RM district, has a typical pluvial river flow regime
450 under oceanic climate influences, where runoff generation is less bounded by evapotranspiration
451 processes,
452 - The Roizonne River basin, in the Alps, typical of summer flow regime controlled by snowmelt, with
453 spring to summer climate conditions dominating changes in low-flows.

454 The visual inspection of response surfaces shows that:

455 - ΔWR* are differently driven by the changes in precipitation Δ*P* and in temperature Δ*T*: ΔWR* is very
456 sensitive to Δ*P* in the Argens River basin (horizontal stratification in the response surface) and to Δ*T* in
457 the Roizonne River basin (vertical stratification in the response surface) whilst being controlled by both
458 drivers in the Ouche River basin;

459 - There is a high likelihood of increase in the duration of water restriction in the Roizonne River basin, as
460 showed a response surface dominated by positive ΔWR*;

461 - *Sd* values may vary significantly from one graph to another (Table 5). For both the Argens and Roizonne
462 River basins, largest *Sd* are found when the response surfaces are displayed with climate variables
463 computed over the whole period April-to-October (AMJJASO) while smallest *Sd* are associated with ΔP
464 and ΔT drivers from March to June. Changes in mean spring to early summer precipitation and
465 temperature mainly govern changes in WR* for these two basins. Conversely changes in precipitation ΔP
466 and temperature ΔT over the full period April-to-October seem the dominant drivers of changes in WR*
467 for the Ouche River basin.

468 **5.2 Response surface analysis at the regional scale**

469 Following (Köplin *et al*. 2012, Prudhomme *et al*. 2013a), the 106 response surfaces were classified to define
470 typical response surfaces, designed as tools to help prioritizing actions for adapting water management rules to
471 future climate conditions in the RM district. Here a hierarchical clustering based on Ward's minimum variance
472 method and Euclidian distance as similarity criteria (Ward 1963) was applied and four classes were identified
473 after inspection of the agglomeration schedule and silhouette plots (Rousseeuw 1987). A manual reclassification
474 was conducted for the few catchments with negative individual silhouette coefficients to ensure higher intra-
475 class homogeneity. For each class, a mean response surface and associated *Sd* was computed, and main climate
476 drivers associated with WR changes identified (Table 5).

477 All suggest an increase in the occurrence of legally-binding water restrictions when precipitation decreases or
478 when temperature increases (Fig. 10). Additional temperature increase and its associated *PET* increase can
479 compensate for precipitation increase and lead to decrease in ΔWR* with intra-class differences emerging in the
480 magnitude of changes. The identified four typical Water Restriction response surfaces show a weak regional
481 pattern and common features. Class 4 (including the Roizonne River basin) regroups snowmelt-fed river flow
482 regimes in the Alps, whilst basins of Class 1 are mainly Mediterranean river flow regimes. Class 2 (including the
483 Ouche River basin) and Class 3 catchments are partly influenced by both precipitation and temperature, with
484 ΔWR* in Class 2 catchments less sensitive to climatic changes (flatter WR response surface) than catchments of
485 Class 3. Flow regime of Classes 2 to 3 ranges from rainfall-fed regimes with high flow in winter and low flow in
486 summer in the northern part of the RM district to regimes partly influenced by snowmelt with high-flows in
487 spring in the Alps and in the Cevennes.

488 To further the regional analysis and help sensitivity assessment at un-modelled catchments, basin descriptors
489 were investigated as possible discriminators of the four classes. A set of potential discriminators - which
490 included measures of the severity, frequency, duration, timing and rate of change in low-flow events (Table 6),
491 the drainage area and the median elevation for the catchment and one climate descriptor (mean annual
492 precipitation and mean annual potential evapotranspiration used to compute an aridity index) – were introduced
493 in a CART model (Classification And Regression Trees, Breiman *et al*., 1984), aimed at performing successive
494 binary splits of a given data set according to decision variables. Through a set of "*if-then*" logical conditions the
495 algorithm automatically identifies the best possible predictors of group membership, starting from the most
496 discriminating decision variable to the less important factors. The optimal choices are fixed recursively by

increasing the homogeneity within the two resulting clusters. At each step one of the clusters (node) is divided into two non-overlapping parts. Here, to free results from catchment size influence, descriptors related to severity were expressed in mm/year, mm/month or mm/day.

Results show three top discriminators, the aridity index being the strongest:

- Aridity index *AI* given by the mean annual precipitation divided by the mean annual potential evapotranspiration (UNEP, 1993),
- Baseflow index *BFI*, a measure of the proportion of the baseflow component to the total river flow, calculated by the separation algorithm separation suggested by Lyne and Hollick (1979),
- Concavity Index *IC* (Sauquet and Catalogne 2011) to characterize the contrast between low-flow and high-flow regimes derived from quantiles of the flow duration curve,

CART overall misclassification (18%) suggests a satisfactory performance in classification method, characterized by a parsimonious algorithm (five nodes and three variables) with potential for a first guess assessment of the WR response to disruptions and evaluation of the robustness of existing water restriction at the department-level scale. For each class, Fig. 11 shows the empirical distribution of the three main discriminators, the mean timing θ of daily discharge below $Q95$ and its dispersion r, based on circular statistics, where $Q95$ is the 95^{th} quantile derived from the flow duration curve.

The classification discriminates catchments primarily on the seasonality of low-flow conditions and the aridity index, with the extreme classes (1 and 4) being particularly well discriminated.

Geographically, Class 1 catchments are mainly located along the Mediterranean coast and include the Argens River basin; ΔWR* is mainly driven by changes in precipitation in spring and early summer. Class 1 gathers water-limited basins with small values of *AI* and a weak sensitivity to climate change in summer. In these dry water-limited basins, the mid-year period exhibits the minimal ratio *P*/*PET* and changes in summer precipitation has hence only a moderate impact on low-flows; spring is the only season when *PET* changes are likely to result in both actual evapotranspiration and discharge changes. WR levels are more likely controlled by antecedent soil moisture conditions in spring and early summer. This behavior is typical of the basins under Mediterranean conditions and was discussed in the context of a scenario-neutral study in Australia (Guo *et al*. 2016). For those catchments, climate drivers computed in spring (over the period MAMJ) are used to describe the x- and y-axes of the response surface, fully consistent with water-limited basin processes.

Catchments of both Class 2 and 3 have similar *IC*, hence suggesting that flow variability is not a proxy for low-flow response to climatic deviation. However, *BFI* values for Class 3 are lower than for Class 2 while Class 3 is characterized by high values for *AI*. Despite higher capability to sustain low-flows (see *BFI* values) the response surface representative of Class 2 is more contrasted than that of Class 3; a possible reason could be drier conditions under current conditions (the median of *AI* equals 2.5 for Class 3 against 1.6 for Class 2). The monthly perturbation factors (see Sect. 5.1) are the same for all the classes but the changes in relative terms are less significant regarding the current climate conditions for Class 3 than for Class 2, and may explain the limited changes in river flow patterns.

Class 4 regroups catchments with low flows in winter and significant snow storage. The *BFI* values are high and due to smooth flow duration curves, *IC* demonstrates also high values.

5.3 Risk assessment at the basin scale

The risk-based framework has been applied to the irrigation water use since annual net total water withdrawal for agriculture purposes is ranked first at the regional scale. Note that in the Rhône-Méditerranée district around 90% and 10% of water used for irrigation originate from surface water and groundwater, respectively. To complement water needs irrigators may also have access to small reservoirs (storage capacity usually less than 1 Mm^3). Most of the reservoirs are filled by surface water in winter and release water later in the following summer. Water restrictions are not imposed to these reservoirs but it is assumed here that during severe drought events the majority of them are empty and thus the existence of potential sources auxiliary to surface water on the conclusions has limited influence on the conclusions.

We assumed here that irrigated farming is globally under failure if the duration with limited or suspended abstraction is above a critical threshold T_c that causes insufficient water for crops. The catchment or area *i* will be considered more vulnerable than the catchment or area *j* if the likelihood of failure (i.e., exceeding T_c) for catchment or area *i* is more than the likelihood of failure for catchment or area *j*. The critical threshold T_c is a value of total number of days with legally-binding water restrictions that needs to be fixed. To move closer to reality and following Simonovic (2010), the value of T_c is based on the analysis of past events. A possible way to fix T_c is to simulate historic drought events observed during the period 2005-2012 and the effects of water restrictions on crop yield and quality and on economic losses. Computing water deficits was considered rather tricky at the farming scale - partly due to the high heterogeneity in crop and soil types, watering systems,

conveyance efficiencies, etc. across the RM district - and we have investigated the use of 'agricultural disaster' notifications as proxies to identify the damaging conditions instead.

Specifically the 'agricultural disaster' notifications are issued by the agriculture ministry following recommendations from the Prefecture to each department affected by extreme hydro-meteorological events, and applied uniformly over the RM district. Whilst 'agricultural disaster' status is a global index that may mask heterogeneity in crop losses within each department, and that reflects losses related to both agricultural and hydrological droughts, it has the advantage of being directly related to economic impact, and uniformly applied across the RM district, hence suitable for a regional-scale analysis. The national system of compensation to farmers is initiated for areas notified under 'agricultural disaster' status.

Over 2005-2012, only one agriculture disaster was declared, in 2011, and applied to 70 of the 95 departments in continental France, and to 16 of the 28 departments fully or partly located in the RM district. Data are collected by the French Ministry of Agriculture and Food and they are not publically available. The year 2011 was the only year when the national system of compensation has been triggered between 1958 and 2013 and the analysis of simulated water restrictions for this year fixed the value for T_c. The duration of water restrictions was calculated individually for each catchment and converted into anomalies $\Delta WR^*(2011)$ with respect to the benchmark value (mean over the period 1958-2013). For consistency with the indicators used in the response surfaces, this threshold $\Delta WR^*(2011)$ is derived from GR6J outputs.

The RCM-based projections of all the catchments of the class for the three time slices 2021-2050, 2041-2070 and 2071-2100 were superimposed to the representative response surfaces to assess the risk of failure (Fig. 4). Finally the vulnerability resulting from the combination of the three components sensitivity, performance and exposure was measured by the proportion of RCM-based projections leading to critical situations , similarly to Prudhomme *et al*. (2015). Technically this Vulnerability Index (*VI*) calculated as the proportion of exposure simulations that fail below the critical threshold T_c is the complement to the "climate-informed" robustness index (*CRI*) (Whateley *et al*., 2014). Given one specific climate projection, a catchment or a group of catchments could be judged vulnerable if on average T_c is exceeded. *VI* is introduced here to account for the uncertainty in climate projections in risk assessment. This index should be interpreted as conditional probability (risk) with respect to a specified ensemble of future climates.

Fig. 12 shows an application to the Ouche River basin, North of the RM district (1, Fig. 1, Table 1) and declared under agricultural disaster status in 2011. The black dotted line are isopleths connecting points of the response surface with $\Delta WR^* = \Delta WR^*(2011) = T_c$ (= 7 10-day periods for this catchment), and delimits the climate space leading to median climatic situations more severe than 2011 ($\Delta WR^* > \Delta WR^*(2011)$, above left) or less severe than 2011 ($\Delta WR^* < \Delta WR^*(2011)$, below right) $\Delta WR^*(2011)$. As reference, the black solid line ($\Delta WR^* = 0$) delimits the climate space associated with more (above left) or less (bottom right) water restrictions compared with the whole period average (1958-2013). Basin-scale exposure projections (Table 2) were plotted onto the WR response surface for three time-slices 2021-2050, 2041-2070 and 2071-2100 (grey symbols), showing a warmer trend but no total precipitation signal. Whilst by the end of the century, projections move towards the critical threshold $\Delta WR^*(2011)$ climate space, pointing out a significant increase in more severe low-flows, there remain a large spread in signal (dispersion of the grey symbols) and the vulnerability index equals zero for this catchment.

5.4 A regional perspective for prioritizing adaptation strategies

Following the methodology applied to the Ouche River basin, $\Delta WR^*(2011)$ were calculated for individual catchments and averaged to produce a value of T_c relevant for each Class (Table 7). Class variation in $\Delta WR^*(2011)$ is large, with Class 2 and 3 showing thresholds of at least 7 10-day periods, whilst they are close to zero for Class 1 and Class 4. The scatter in the $\Delta WR^*(2011)$ values is certainly due to heterogeneity in crops, in irrigation systems, in climate conditions, etc. at the regional scale leading to locally differentiated sensitivity to water restrictions as well as to biases in WR modelling. Since only the year 2011 it is now difficult to conclude on the origins of the dispersion (natural or non-natural). However the distribution and absolute values of the critical thresholds reflect well the spatial pattern of WR enforced from May to September 2011, with Southern regions and the French Alps moderately affected by lack of rainfall in spring compared to the Northern and Western regions of the RM district (Fig. 13). Surprisingly negative values for $\Delta WR^*(2011)$ are found for some catchments of Classes 1 and 4, providing no evidence to support their agricultural disaster status that year. At the RM scale, average $\Delta WR^*(2011)$ equals 38 days when considering all catchments, and increases to 66 days when considering only catchments under agricultural disaster status. Simplifying but realistic assumptions are imposed by the lack of detail information; thus only one value was considered at the regional scale despite high dispersion in $\Delta WR^*(2011)$ values (Table 7): the critical threshold T_c was set to the average of the $\Delta WR^*(2011)$ values computed on all catchments in departments under agricultural disaster status in 2011 (6.6 10-day periods), and

was used thereafter for all classes. Note that this value of T_c seems realistic: it represents a significant period with restrictions (66 days or 30% of the time between the 1st April and the 31st October).

Using the Class WR response surface as diagnostic tools, exposure information (grey symbols) and thresholds (ΔWR*=0, solid, ΔWR*(2011), dashed black lines) were displayed (Fig. 14), and *VI* calculated (Table 7). The location of the two isopleths ΔWR*= ΔWR*(2011) (black dotted line) and ΔWR*= 0 (black straight line) in the WR response surface depends on the shape of the response surface and differ from one class to another. The portion of the WR response surface associated with ΔWR*<0 is gradually lower from Class 1 to Class 4 suggesting that catchments of Class 4 are more subject to an increase in water restriction occurrence than catchments of the other classes. Classes 1 and 4, the most extreme responses classes, contain fewer catchments, whilst Classes 2 and 3, characterized by an intermediate response, have the most of the catchments. Because of the large geographical spread of catchments of Class 2 and 3, an expert-based division was done to distinguish catchments with continental (northern sectors) and Mediterranean (southern sectors) climate in terms of exposure. This is to better capture the predominantly north–south gradient in future projections of both temperature and rainfall, as they differing impact on the river flow regime (*e.g.*, Boé *et al*. 2009; Chauveau *et al*. 2013; Dayon *et al*. 2018). For all classes, vulnerability increases with lead time, with Class 4 showing the largest vulnerability and Class 1 being the less vulnerable despite its location in the Mediterranean area. In the two classes 2 and 3, vulnerability increases from North to South in the RM district (*e.g.*, *VI* = 13% for Class 2-N against 32.9% for Class 2-S at the end of the century). These contrasted results are mainly explained by the difference between exposure characterizations since a common value of the threshold T_c was adopted.

These preliminary results may support recent initiatives taken at different scales to develop adaption strategies to climate change are developing in France:

- In 2011, France adopted a general framework for action—the French National Climate Change Impact Adaptation Plan ("Plan National d'Adaptation au Changement Climatique (PNACC)" in French)—with numerous recommendations related to research and observation. Five priorities of the first PNACC related to water resources have been highlighted. The PNACC has been recently reviewed and the PNACC2 published in December 2018 confirms the place of DMPs as tools for monitoring water resources and water allocation, and for driving greater public and stakeholder awareness. Results here show that the climate change effects could be felt more acutely during the irrigation period by an increase in water restriction, relying on surface water to compensate deficits is highly hazardous, current agricultural practices should be

revised (probably in catchments of Class 4 from the short perspective, and later for the other areas) and any change in the current DMPs should be examined in terms of consequence for all uses.

- The RM Water Agency has initiated an unprecedented major initiative that provides guidance for the River Basin Management Plan (2016–2021). The strategy partly relies on an analysis of the vulnerability in different water-related sectors (water resources, soil-moisture, biodiversity, and water quality) within the RM district to climate change. The study here complements this analysis by focusing on agricultural uses and introducing the bottom-up concept.

6 Conclusions

This paper presents a first attempt to analyse and simulate water restrictions over a large area in France applying an alternative approach to the classical "top-down" approach. The risk-based approach developed here relies on sensitivity-based analyses to a wide range of climate changes, making it scenario-neutral. However ex ante climate projections are introduced in the last stage of the framework to assess the likelihood of failure.

The analysis of the past and current DMPs in the RM district shows a decision-making processes highly heterogeneous both in terms of low-flow monitoring variable and regulatory thresholds. In reality, the WR statements follow a set of rules defined in the DMPs (which can be simulated and reproduced automatically) but also expert judgment or lobbying from key stakeholders - which are not accounted for in the WRL modelling framework put in place here. However, the post-processing of GR6J outputs allows detecting more than 68% of severe alerts (more severe than level 1), making the developed framework a useful tool. Our study is a first step towards a comprehensive accounting of physical processes, but does not capture socio-economic factors, also critically important and reaches out to interdisciplinary for completing the modelling framework designed here. The study at the regional scale illustrates an expected difficulty to simulate accurately a regulatory framework. Further improvement is not expected in enhancing hydrological models but in reproducing decision-making processes. The overall performance could be improved by scrutinizing the minutes of the drought committees to better understand the weight of the stakeholders in the final statement.

The sensitivity analysis and the related response surfaces suggest that basins located in the Southern Alps are the most responsive basins to climate change and that those experiencing a high ratio *P/PET* are found the less responsive. The classification method CART has been applied to 106 responses surfaces associated with 106 gauged basins and leads to four classes with different sensitivity. The key-variables known at un-modelled but gauged catchments can be introduced in the decision-tree to finally predict the assignment as a first guess to one

667 of the four classes. Water managers are thus encouraged to monitor in priority and more accurately temperature
668 and/or precipitation when and where the sensitivity of their catchments is found the highest. This may mean
669 efforts to reinforce field instrumentation within these key catchments, but also an opportunity to implement
670 awareness and participatory methods to initiate or to consolidate dialogues between stakeholders from a long
671 term perspective.

672 The impact of climate change on the river flow is expected to be gradual, thus offering opportunities to update,
673 to harmonize and to adapt Drought Management Plans to changes in climate conditions and water needs. As a
674 consequence, the need for adaptation of existing drought action plans could differ much from one catchment to
675 another and should take into account intrinsic sensibility to climate change besides 'top-down' projections.
676 Results also show needs to firstly adapt DMPs in temperature sensitive catchments more subject to a significant
677 increase in legally-binding restrictions in the short term. In contrast, the capacity to anticipate new regulations
678 will be challenging where water restrictions are largely driven by precipitation. Regarding long-term relevance
679 of DMPs, robustness of DMPs in these catchments is not warranted given the large uncertainties in precipitation
680 regional projections.

681 The risk-based approach was applied to assess the vulnerability of irrigation due to regulatory instruments
682 under modified climate. Evaluating the impact of climate change on irrigation was not the objective of the
683 suggested framework; it has been applied to estimate the likelihood of failure for irrigation at various lead times,
684 instead. Usually, a failure can be stated when irrigation water needs are not fully satisfied. This case study
685 suggests the use of a proxy obtained from a national system of compensation to define a critical threshold
686 (maximum acceptable duration with water restriction). Analysis, however, was based on limited data (one year)
687 and a better failure assessment is required using other years (e.g., 2015 and 2017. The higher the probability, the
688 more vulnerable the irrigation use within the department. Finally, socio-economic system stressors like
689 agricultural practices, population growth, water demand, etc. should be considered to highlight combinations that
690 would lead to unacceptable conditions and to assess the performance of various adaptation strategies under an
691 extended set of future climate conditions (Poff *et al*. 2016).

692 Climate response surface appears as a convenient tool for simulating and discussing future perspectives locally
693 on the basin scale or more broadly on a given management territory. For example, they can support implement
694 adaptive strategies (see - as an example - the Robust Decision Making framework suggested by Lempert and
695 Groves (2010)): response surfaces can be drawn for different adaptation scenarios combined with periodic

updates of DMPs including rules for defining regulatory thresholds and monitoring variables evolving over time, etc.

Note that all results are based on a single hydrological model, but a multi-model approach could be applied as the magnitude of the rainfall-runoff response was shown vary with different hydrological models (*e.g.*, Vidal *et al*. 2016; Kay *et al.* 2014). Finally, an extension of the area of interest to the whole France may bring to light a more complete typology of response surfaces and a wider range of sensitivity.

Acknowledgments

The authors thank Météo-France for providing access to the Safran database. Regional projections were obtained from the DRIAS portal (http://drias-climat.fr/) and consulted on November 2016. Analyses were performed in R (R Core Team 2016) with packages airGR (Coron *et al.* 2017), chron (James and Hornik 2017), circular (Lund *et al*., 2017), doParallel (Calaway *et al*. 2017), dplyr (Wickham and François 2015), ggplot2 (Wickham 2009), hydroTSM (Zambrano-Bigiarini 2014), RColorBrewer (Neuwirth 2014), reshape2 (Wickham 2007), rpart (Therneau *et al*. 2018), scales (Wickham 2016), stringr (Wickham 2017) and zoo (Zeileis and Grothendieck 2005). The study was funded by Irstea and the French RM Water Agency.

References

Andrew J.T. and Sauquet E.: Climate Change Impacts and Water Management Adaptation in Two Mediterranean-Climate Watersheds: Learning from the Durance and Sacramento Rivers. Water 2017, 9, 126, doi: 10.3390/w9020126, 2017.

Arnell N.W.: Relative effects of multi-decadal climatic variability and changes in the mean and variability of climate due to global warming: future streamflow in Britain. J. Hydrol. 270, 19–213, 2003.

Barbier R., Barreteau O., and Breton C.: Management of water scarcity: between negotiated implementation of the “décret sécheresse” and emergence of local agreements. Ingénieries - EAT IRSTEA édition 2007, 3-19, 2007.

Bisselink B., Bernhard J., Gelati E., Adamovic M., Guenther S., Mentaschi L. and De Roo A.: Impact of a changing climate, land use, and water usage on Europe’s water resources, EUR 29130 EN, Publications Office of the European Union, Luxembourg, 2018, ISBN 978-92-79-80287-4, doi:10.2760/847068, JRC110927, 2018.

722 Boé J., Terray L., Martin E., and Habets F.: Projected changes in components of the hydrological cycle in French
723 river basins during the 21st century. Water Resour. Res. 45 (8), W08426, doi:10.1029/2008WR007437, 2009.
724 Breiman L., Friedman J.H., Olshen R., and Stone C.J.: Classification and Regression Trees, Wadsworth,
725 Belmont, California, 1984.
726 Brekke L.D., Maurer E.P., Anderson J.D., Dettinger M.D., Townsley E.S., Harrison A., and Pruitt T.: Assessing
727 reservoir operations risk under climate change. Water Resour. Res., 45, W04411, doi:10.1029/2008WR006941,
728 2009.
729 Broderick C., Murphy C., Wilby R.L., Matthews T., Prudhomme C., and Adamson, M. (2019). Using a Scenario
730 - neutral framework to avoid potential maladaptation to future flood risk. Water Resources Research, 55.
731 https://doi.org/10.1029/2018WR023623
732 Brown C., Werick W., Leger W., and Fay D.: A decision-analytic approach to managing climate risks:
733 Application to the upper great lakes. Journal of the American Water Resources Association (JAWRA) 47, 524–
734 534, 2011.
735 Brown C., Ghile Y., Laverty M., and Li K.: Decision scaling: Linking bottom-up vulnerability analysis with
736 climate projections in the water sector. Water Resour. Res. 48, W09537, doi:10.1029/2011WR011212, 2012.
737 Brown C., Wilby R.L.: An alternate approach to assessing climate risks. Trans. Am. Geophys. Union 93(41),
738 401–402, 2012.
739 Bubnová R., Hello G., Bénard P., and Geleyn J.F.: Integration of the Fully Elastic Equations Cast in the
740 Hydrostatic Pressure Terrain-Following Coordinate in the Framework of the ARPEGE/Aladin NWP System.
741 Monthly Weather Review 123 (2), 515-35, 1995.
742 Caillouet L., Vidal J.-P., Sauquet E., Devers A., and Graff B: Ensemble reconstruction of spatio-temporal
743 extreme low-flow events in France since 1871. Hydrol. Earth Syst. Sci. 21, 2923-2951, 2017.
744 Calaway R., Microsoft Corporation, Weston S., and Tenenbaum D.: doParallel: Foreach Parallel Adaptor for the
745 'parallel' Package. R package version 1.0.11, https://CRAN.R-project.org/package=doParallel, 2017.
746 Chauveau M., Chazot S., Perrin C., Bourgin P.-Y., Sauquet E., Vidal J.-P., Rouchy N., Martin E., David J.,
747 Norotte T., Maugis P., and de Lacaze X: What will be the impacts of climate change on surface hydrology in
748 France by 2070? La Houille Blanche 4, 5-15, 2013.
749 Cipriani T., Tilmant F., Branger F., Sauquet E., and Datry T. : Impact of climate change on aquatic ecosystems
750 along the Asse river network. In “Hydrology in a Changing World: Environmental and Human Dimensions”
751 (Daniell T., Ed.), AIHS Publ. 363, 2014, 463-468, 2014.

752 Collet L., Harrigan S., Prudhomme C., Formetta G., and Beevers L.: Future hot-spots for hydro-hazards in Great
753 Britain: a probabilistic assessment, Hydrol. Earth Syst. Sci., 22, 5387-5401, https://doi.org/10.5194/hess-22-
754 5387-2018, 2018.
755 Coron L., Thirel G., Delaigue O., Perrin C., and Andréassian V.: airGR: A Suite of Lumped Hydrological
756 Models in an R-Package. Environmental Modelling and Software 94, 166-171,
757 https://doi.org/10.1016/j.envsoft.2017.05.002, 2017.
758 Culley S., Noble S., Yates A., Timbs M., Westra S., Maier H.R., Giuliani M., and Castelletti A.: A bottom-up
759 approach to identifying the maximum operational adaptive capacity of water resource systems to a changing
760 climate. Water Resour. Res. 52, 6751–6768, 2016.
761 Danner A., Mohammad Safeeq G., Grant GE., Wickham C., Tullos D., and Santelmann M.V.: Scenario-Based
762 and Scenario-Neutral Assessment of Climate Change Impacts on Operational Performance of a Multipurpose
763 Reservoir. Journal of the American Water Resources Association (JAWRA) 53(6), 1467-1482, 2017.
764 Dayon G., Boé J., Martin E., and Gailhard J.: Impacts of climate change on the hydrological cycle over France
765 and associated uncertainties. Comptes Rendus Geoscience 350(4), 141-153, 2018.
766 Fronzek S., Carter T.R., and Räisänen J.: Applying probabilistic projections of climate change with impact
767 models: a case study for sub-arctic palsa mires in Fennoscandia. Climatic Change 99, 515–534, 2010.
768 Ghile Y.B., Taner M.Ü., Brown C., and Talbi A.: Bottom-up climate risk assessment of infrastructure investment
769 in the Niger River Basin. Climatic Change 122(1–2), 97–110, 2014.
770 Giorgi F.: Climate change hot-spots. Geophys. Res. Lett., 33, L08707, doi:10.1029/2006GL025734, 2006.
771 Guo D., Westra S., and Maier H.R.: An inverse approach to perturb historical rainfall data for scenario-neutral
772 climate impact studies. J. Hydrol. 556: 877-890, 2016.
773 Guo D., Westra S., and Maier H.R.: Use of a scenario-neutral approach to identify the key hydrometeorological
774 attributes that impact runoff from a natural catchment. J. Hydrol.
775 http://dx.doi.org/10.1016/j.jhydrol.2017.09.021, 2017.
776 Gupta, H. V., Kling, H., Yilmaz, K., and Martinez, G. F.: Decomposition of the mean squared error and NSE
777 performance criteria: Implications for improving hydrological modelling, J. Hydrol., 377, 80–91,
778 https://doi.org/10.1016/j.jhydrol.2009.08.003, 2009.
779 Hellwig J. and Stahl K.: An assessment of trends and potential future changes in groundwater-baseflow drought
780 based on catchment response times, Hydrol. Earth Syst. Sci., 22, 6209-6224, https://doi.org/10.5194/hess-22-
781 6209-2018, 2018.

Hublart P., Ruelland D., García de Cortázar-Atauri I., Gascoin S., Lhermitte S., and Ibacache A.: Reliability of lumped hydrological modeling in a semi-arid mountainous catchment facing water-use changes. Hydrol. Earth Syst. Sci. 20, 3691-3717, https://doi.org/10.5194/hess-20-3691-2016, 2016.

Jacob D., Petersen J., Eggert B., Alias A., Christensen O.B., Bouwer L.M., and Braun A.: EURO-CORDEX: New high-resolution climate change projections for European impact research, Regional environmental change 14(2), 563-78, 2014.

James D. and Hornik K.: chron: Chronological Objects which Can Handle Dates and Times. R package version 2.3-50, https://CRAN.R-project.org/package=chron, 2017.

Jiménez Cisneros B.E., Oki T., Arnell N.W., Benito G., Cogley J.G., Döll P., Jiang T., and Mwakalila S.S.: Freshwater resources. In: Climate Change 2014: Impacts, Adaptation, and Vulnerability. Part A: Global and Sectoral Aspects. Contribution of Working Group II to the Fifth Assessment Report of the Intergovernmental Panel on Climate Change [Field, C.B., V.R. Barros, D.J. Dokken, K.J. Mach, M.D. Mastrandrea, T.E. Bilir, M. Chatterjee, K.L. Ebi, Y.O. Estrada, R.C. Genova, B. Girma, E.S. Kissel, A.N. Levy, S. MacCracken, P.R. Mastrandrea, and L.L. White (eds.)]. Cambridge University Press, Cambridge, United Kingdom and New York, NY, USA, 229-269, 2014.

Jolliffe I.T. and Stephenson D.B.: Forecast verification. A practitioner's Guide in Atmospheric Science. John Wiley & Sons Edition, 2003.

Kay A. L., Crooks S. M., and Reynard N. S.: Using response surfaces to estimate impacts of climate change on flood peaks: assessment of uncertainty. Hydrol. Process., 28, 5273–5287, https://doi.org/10.1002/hyp.10000, 2014.

Köplin N., Schädler B., Viviroli D., and Weingartner R.: Relating climate change signals and physiographic catchment properties to clustered hydrological response types. Hydrol. Earth Syst. Sci. 16: 2267–2283, 2012.

Lémond J., Dandin P., Planton S., Vautard R., Pagé C., Déqué M., Franchistéguy L., Geindre S., Kerdoncuff M., Li L., Moisselin J.M., Noël T., and Tourre Y.M.: DRIAS: a step toward Climate Services in France. Adv. Sci. Res. 6: 179-186, 2011.

Lempert R.J., and Groves D.G.: Identifying and evaluating robust adaptive policy responses to climate change for water management agencies in the American west. Technological Forecasting and Social Change 77(6): 960-974, https://doi.org/10.1016/j.techfore.2010.04.007, 2010.

Lund U., Agostinelli C., Arai H., Gagliardi A., Garcia Portugues E., Giunchi D., Irisson J.O., Pocernich M., and Rotolo F.: circular: Circular Statistics. R package version 0.4-93, https://CRAN.R-project.org/package=circular, 2017.

Lyne V. and Hollick M.: Stochastic time variable rainfall runoff modeling. In: Proceedings of the Hydrology and Water Resources Symposium Berth, 1979. National Committee on Hydrology and Water Resources of the Institution of Engineers, Australia, 89–92, 1979.

Mastrandrea M.D., Heller N.E., Root T.L., and Schneider S.H.: Bridging the gap: linking climate-impacts research with adaptation planning and management. Climatic Change 100, 87-101, 2010.

MEDDE - Ministère de l'Ecologie et du Développement Durable (2004) Plan d'Action Sécheresse.

Nash J.E. and Sutcliffe J.V.: River flow forecasting through conceptual models Part I – A discussion of principles. J. Hydrol. 10(3), 282–290, 1970.

Neuwirth E.: RColorBrewer: ColorBrewer Palettes. R package version 1.1-2, https://CRAN.R-project.org/package=RColorBrewer, 2014.

Oudin L., Hervieu F., Michel C., Perrin C., Andréassian V., Anctil F., and Loumagne C.: Which potential evapotranspiration input for a lumped rainfall–runoff model?: Part 2 — towards a simple and efficient potential evapotranspiration model for rainfall– runoff modelling. J. Hydrol. 303, 290–306, 2005.

Paeth H., Vogt G., Paxian A., Hertig E., Seubert S., and Jacobeit J.: Quantifying the evidence of climate change in the light of uncertainty exemplified by the Mediterranean hot spot region. Global and Planetary Change 151, 144-151, 2017.

Paton F., Maier H., and Dandy G.: Relative magnitudes of sources of uncertainty in assessing climate change impacts on water supply security for the southern Adelaide water supply system. Water Resour. Res. 49(3), 1643–1667, 2013.

Perrin C., Michel C., and Andréassian V. Improvement of a parsimonious model for streamflow simulation. J. Hydrol. 279, 275–289, 2003.

Poff N.L., Brown C.M., Grantham T.E., Matthews J.H., Palmer M.A., Spence C.M., Wilby R.L., Haasnoot M., Mendoza G.F., Dominique K.C., and Baeza A.: Sustainable water management under future uncertainty with eco-engineering decision scaling. Nature Climate Change 6(1), 25-34, 2016.

Poncelet C., Merz R., Merz B., Parajka J., Oudin L., Andréassian V., and Perrin C.: Process-based interpretation of conceptual hydrological model performance using a multinational catchment set. Water Resour. Res. 53, 7247–7268, 2017.

Pushpalatha R., Perrin C., Le Moine N., Mathevet T., and Andréassian V. A downward structural sensitivity analysis of hydrological models to improve low-flow simulation. J. Hydrol. 411, 66–76, 2011.

Prudhomme C., Wilby R.L, Crooks S., Kay A.L. and Reynard N.S.: Scenario-neutral approach to climate change impact studies: Application to flood risk. J. Hydrol. 390(3–4), 198-209, 2010.

.

Prudhomme C., Kay A., Crooks S., and Reynard N.: Climate change and river flooding: Climate change and river flooding: Part 1 classifying the sensitivity of British catchments. Climatic Change 119, 933-948, 2013a.

Prudhomme C., Kay A., Crooks S., and Reynard N. Climate change and river flooding: Part 2 sensitivity characterization for British catchments and example vulnerability assessments. Climatic Change 119, 949–964, 2013b.

Quintana-Seguí P., Le Moigne P., Durand Y., Martin E., Habets F., Baillon M., Canellas C., Franchistéguy L., and Morel S.: Analysis of near-surface atmospheric variables: validation of the safran analysis over France. J. Appl. Meteorol. Clim. 47, 92–107, 2008.

Radnoti G.: Comments on A Spectral Limited-Area Formulation with Time-Dependent Boundary Conditions Applied to the Shallow-Water Equations. Monthly Weather Review 123:2, 1995.

R Core Team: R: A Language and Environment for Statistical Computing, R Foundation for Statistical Computing, Vienna, Austria, https://www.R-project.org/, 2016.

Ray P.A. and Brown C.M. Confronting Climate Uncertainty in Water Resources Planning and Project Design: The Decision Tree Framework. Washington, DC: World Bank, 2015.

Rousseeuw P.J. Silhouettes: A graphical aid to the interpretation and validation of cluster analysis. Journal of Computational and Applied Mathematics 20 (November), 53-65, 1987.

Samaniego L.,Thober S.,Kumar R.,Wanders N.,Rakovec O.,Pan M.,Zink M.,Sheffield J.,Wood E.F., and Marx, A.: Anthropogenic warming exacerbates European soil moisture droughts. Nature Climate Change 8(5), 421-426, https://doi.org/10.1038/s41558-018-0138-5, 2018.

Sauquet E.: Mapping mean annual river discharges: geostatistical developments for incorporating river network dependencies. J. Hydrol. 331, 300–314, 2006.

Sauquet E., Gottschalk L., and Krasovskaia I.: Estimating mean monthly runoff at ungauged locations: an application to France. Hydrology Research 39(5-6), 403-423, 2008.

Sauquet E. and Catalogne C.: Comparison of catchment grouping methods for flow duration curve estimation at ungauged sites in France. Hydrol. Earth Syst. Sci. 15, 2421–2435, 2011.

Sauquet E., Arama Y., Blanc‐Coutagne E., Bouscasse H., Branger F., Braud I., Brun J.-F., Cherel J., Cipriani T., Datry T., Ducharne A., Hendrickx F., Hingray B., Krowicki F., Le Goff I., Le Lay M., Magand C., Malerbe F., Mathevet T., Mezghani A., Monteil C., Perrin C., Poulhe P., Rossi A., Samie R., Strosser P., Thirel G., Tilmant F., and Vidal J.-P.: Water allocation and uses in the Durance River basin in the 2050s: Towards new management rules for the main reservoirs?, La Houille Blanche 5, 25-31, 2016.

Schlef K.E., Steinschneider S., and Brown C.M.: Spatiotemporal Impacts of Climate and Demand on Water Supply in the Apalachicola-Chattahoochee-Flint Basin. J. Water Resour. Plann. Manage., 2018, 144(2): 05017020, 2018.

Simonovic S.P.: A new methodology for the assessment of climate change impacts on a watershed scale. Current Science 98(8), 1047-1055, 2010.

Singh R., Wagener T., Crane R., Mann M.E., and Ning L.: A vulnerability driven approach to identify adverse climate and land use change combinations for critical hydrologic indicator thresholds: application to a watershed in Pennsylvania, USA. Water Resour. Res. 50(4), 3409–3427, 2014.

Skamarock W., Klemp J., Dudhia J., Gill D., Barker D., Wang W., Huang X.-Y., and Duda M.: A description of the advanced research WRF version 3, doi:10.5065/D68S4MVH, 2008.

Steinschneider S. and Brown C.M.: A semiparametric multivariate, multisite weather generator with low-frequency variability for use in climate risk assessments, Water Resour. Res., 49, 7205–7220, doi:10.1002/wrcr.20528, 2013.

Terray L. and Boé J.: Quantifying 21st-century France climate change and related uncertainties. Comptes Rendus Geoscience, 345, 136–149, 2013.

Therneau T., Atkinson B., and Ripley B. rpart: Recursive Partitioning and Regression Trees. R package version 4.1-13, https://CRAN.R-project.org/package=rpart, 2018.

Touma D, Ashfaq M, Nayak M.A., Kao S.-C., Diffenbaugh N.S.: A multi-model and multi-index evaluation of drought characteristics in the 21st century. J. Hydrol., 526, 196-207, 2015

Van Loon A.F., Gleeson T., Clark J., Van Dijk A.I.J.M., Stahl K., Hannaford J., Di Baldassarre G., Teuling A.J., Tallaksen L.M., Uijlenhoet R., Hannah D.M., Sheffield J., Svoboda M., Verbeiren B., Wagener T., Rangecroft S., Wanders N., and Van Lanen H.A.J.: Drought in the Anthropocene, Nature Geoscience, 9, 89-91, 2016.

Taylor K.E., Stouffer R.J., and Meehl G.A.: An overview of CMIP5 and the experiment design. Bull. Am. Meteorol. Soc. 93(4), 485-498, 2012.

Valéry A., Andréassian V., and Perrin C.: 'As simple as possible but not simple': What is useful in a temperature-based snow-accounting routine? Part 2 - Sensitivity analysis of the Cemaneige snow accounting routine on 380 catchments. J. Hydrol. 517, 1176–1187, 2014.

Vidal J.-P., Martin E., Franchistéguy L., Baillon M, and Soubeyroux J.-M.: A 50-year high-resolution atmospheric reanalysis over France with the Safran system. Int. J. Clim. 30, 1627–1644, 2010.

Vidal J.-P., Hingray B., Magand C., Sauquet E., and Ducharne A.: Hierarchy of climate and hydrological uncertainties in transient low-flow projections. Hydrol. Earth Syst. Sci. 20, 3651–3672, 2016.

Ward J. Jr.: Hierarchical grouping to optimize an objective function. Journal of the American Statistical Association 58(301), 236-44, 1963.

Whateley S., Steinschneider S., and Brown C.M.: A climate change range-based method for estimating robustness for water resources supply. Water Resour. Res. 50, 8944–8961, 2014.

Weiß M.: Future water availability in selected European catchments: a probabilistic assessment of seasonal flows under the IPCC A1B emission scenario using response surfaces. Nat Hazards Earth Syst Sci 11:2163–2171, 2011.

Wetterhall F., Graham L.P., Andréasson J., Rosberg J., and Yang W. Using ensemble climate projections to assess probabilistic hydrological change in the nordic region. Natural Hazards and Earth System Sciences 11, 2295–2306, 2011.

Wickham H.: ggplot2: Elegant Graphics for Data Analysis, Springer-Verlag New York, http://ggplot2.org, 2009.

Wickham H. and Francois R. dplyr: A Grammar of Data Manipulation. R package version 0.4.3, https://CRAN.R-project.org/package=dplyr, 2015.

Wickham H.: scales: Scale Functions for Visualization. R package version 0.4.0, https://CRAN.R-project.org/package=scales, 2016.

Wickham H.: stringr: Simple, Consistent Wrappers for Common String Operations. R package version 1.2.0, https://CRAN.R-project.org/package=stringr, 2017.

Wickham H.: stringr: Simple, Consistent Wrappers for Common String Operations. R package version 1.2.0. https://CRAN.R-project.org/package=stringr, 2017.

Zambrano-Bigiarini M.: hydroTSM: Time series management, analysis and interpolation for hydrological modelling. R package version 0.4-2-1. https://CRAN.R-project.org/package=hydroTSM, 2014.

Zeileis A. and Grothendieck G.: zoo: S3 Infrastructure for Regular and Irregular Time Series. Journal of Statistical Software, 14(6), 1-27. doi:10.18637/jss.v014.i06, 2005.

929

N°	River basin	Department (department number)	Station number	Elevation (m.a.s.l.)	Area (km^2)	Regime class	NSE_{LOG}	KGE_{SQRT}
1	Ouche	Côte d'Or (21)	U1324010	243	651	6	0.84	0.94
2	Bourbre	Isère (38)	V1774010	202	703	1	0.85	0.92
3	Roizonne	Isère (38)	W2335210	936	71.6	11	0.71	0.84
4	Bonne	Isère (38)	W2314010	770	143	12	0.80	0.91
5	Buëch	Hautes-Alpes (05)	X1034020	662	723	9	0.84	0.93
6	Drôme	Drôme (26)	V4214010	530	194	3	0.81	0.89
7			V4264010	263	1150	9	0.85	0.88
8	Roubion	Drôme(26)	V4414010	264	186	9	0.83	0.93
9	Lot	Lozère (48)	O7041510	663	465	3	0.88	0.94
10	Tarn	Lozère (48)	O3011010	905	67	8	0.73	0.90
11			O3031010	565	189	9	0.81	0.91
12	Hérault	Hérault (34)	Y2102010	126	912	8	0.83	0.88
13	Asse	Alpes de Haute-Provence (04)	X1424010	605	375	9	0.80	0.86
14	Caramy	Var (83)	Y5105010	172	215	2	0.85	0.94
15	Argens	Var (83)	Y5032010	175	485	2	0.80	0.92

Table 1: Main characteristics of the 15 catchments used for validation of water restriction simulations. Station number refers to the catchment number in the HYDRO database and regime class to the classification suggested by Sauquet *et al.* (2008) with a gradient from Class 1- pluvial fed regime moderately contrasted to Class 12- snowmelt fed regime.

Data source	Representative Concentration Pathway			Reference
	RCP2.6	RCP4.5	RCP8.5	
ALADIN	A	A	NA	Bubnová et al. (1995). Radnoti (1995)
First quartile, median and last quartile of the ensemble EURO-CORDEX results	NA	A	A	Jacob et al. (2014)
WRF	NA	A	NA	Skamarock et al. (2008)

Table 2: Regional climate projections available in the DRIAS portal (A: available; NA: not available).

Level	Name	Water restriction							
		Recreational	Vehicle washing	Lawn watering	Swimming-pool filling	Urban washing	Irrigation	Industry	Drinking water and sanitation
0	Vigilance	×	×	×	×	×			
1	Alert	×	×	×	×	×	×	×	
2	Reinforced alert	×	×	×	×	×	×	×	
3	Crisis	×	×	×	×	×	×	×	×

Table 3: Uses affected by water restriction according to the drought severity

WR* event		WR level ≥ 1 (Benchmark)	
		Yes	*No*
WR level ≥ 1 (Prediction)	*Yes*	hits	false alarms
	No	misses	correct negatives

Table 4: Contingency table for legally-binding restriction (WR*).

941

	Sd	Period		
		AMJJASO	JASO	MAMJ
Argens River basin (Class 1)	median	1.59	1.65	**0.19**
	max	3.32	3.69	**1.21**
Ouche River basin (Class 2)	median	**0.63**	0.78	1.10
	max	**1.03**	1.52	1.99
Roizonne River basin (Class 4)	median	1.12	1.32	**0.64**
	max	1.98	2.49	**0.91**
All	median	**0.69**	0.80	0.70
	max	1.45	1.70	**1.24**
Class 1	median	1.16	1.24	**0.25**
	max	2.70	2.96	**1.17**
Class 2	median	**0.72**	0.85	0.89
	max	1.45	1.81	**1.43**
Class 3	median	**0.41**	0.49	0.64
	max	**0.88**	0.97	1.06
Class 4	median	0.91	1.14	**0.81**
	max	1.78	2.15	**1.28**

942 **Table 5: Summary statistics for standard deviation *Sd* of the grid for different axes.**

943

944

Component of the river flow regime	Hydrological indices
Severity	Flow exceeded 95% of the time ($Q95$) Annual minimum 10-day daily mean low flow with a 5-year recurrence interval Annual maximum deficit below threshold Q95 exceeded 20% of time
Duration	Annual maximum maximal duration of the continuous sequence of zero flow within the year, exceeded on average every five years ($D80$). Maximum duration of consecutive zero flows (D) are sampled by block maxima approach and $D80$ is defined as the empirical 80th percentile of cumulative distribution function of D Seasonal recession time scales (DT and $Drec$). This duration based on the hydrograph defined by the 1-day and 30-day moving average of the 365 long term mean daily discharges, d= 1,…, 365 (Qd and $Q30d$, respectively). $Drec$ is defined by the time lapse between the median $Qd50$ and the 90th quantile $Qd90$ of Qd on the falling limb of the hydrograph defined by $Q30d$ and $DT = \ln(Qd50/Qd90)/Drec$
Rate of Change	Ratio $Q95/Q50$ Concavity index derived from flow duration curve $(Q10 - Q99)/(Q1 - Q99)$ (Sauquet and Catalogne, 2011). This descriptor is a dimensionless measure of the contrast between low-flow and high-flow regimes derived from quantiles of the flow duration curve Baseflow index (BFI). BFI is a measure of the proportion of the baseflow component to the total river flow, calculated by the separation algorithm separation suggested by Lyne and Hollick (1979) Class of river flow regime based on average monthly runoff pattern defined by Sauquet *et al.* (2008) (between 1 and 12) Seasonality ratio (SR) $SR = Q95_{AMJJASON}/Q95_{DJFM}$ ($SR > 1$ for mountainous catchment) with $Q95_{AMJJASON}$ and $Q95_{DJFM}$ computed on seasonal flow duration curves
Frequency	Proportion of years with at least one value below $Q95$
Timing	Mean day of first occurrence of flow below $Q95$ Mean and dispersion of the occurrence of flows below $Q95$ within the year (θ and r, $rsin(\theta)$ and $rcos(\theta)$. These two variables are circular statistics. Each day i with zero flow is converted into an angular (t_i) and represented by a unit vector with rectangular coordinates ($cos(t_i)$; $sin(t_i)$). The mean of the cosines and sines defines a representative vector. The value for θ is obtained by calculating the inverse tangent of the angle of the mean vector and the norm of the mean vector provides a measure of the regularity in the dates (a value close to one indicates a high concentration around θ while a value close to zero indicates no seasonality)

945 **Table 6: Hydrological metrics considered to investigate similarity in CART.**

946

Class		Number of catchments (with agricultural disaster status)	Mean ΔWR*(2011) (with agricultural disaster status) (× 10 days)	Vulnerability index *VI* (%)		
				2021-2050	2041-2070	2071-2100
1	**All**	**15 (2)**	**-1.2 (-2.3)**	**6.1**	**11.5**	**6.7**
2	**All**	**44 (22)**	**5.0 (7.1)**	**6.4**	**11.8**	**21.6**
	N	25 (18)	6.1 (6.2)	0	0	13
	S	19 (4)	3.4 (11.3)	14.8	27.3	32.9
3	**All**	**38 (13)**	**5.4 (8.7)**	**1.7**	**4.5**	**7.9**
	N-E	25 (4)	3.7 (3.8)	0.4	0	4.5
	S-W	13 (9)	8.5 (10.8)	4.19	13.3	14.4
4	**All**	**9 (3)**	**0 (-0.7)**	**18.2**	**45.4**	**47.2**
All		**106 (40)**	**3.8 (6.6)**	**5.8**	**12**	**16.7**

Table 7: Summary statistics for the mean anomaly ΔWR*(2011) and for the measure of vulnerability *VI* estimated at the regional scale.

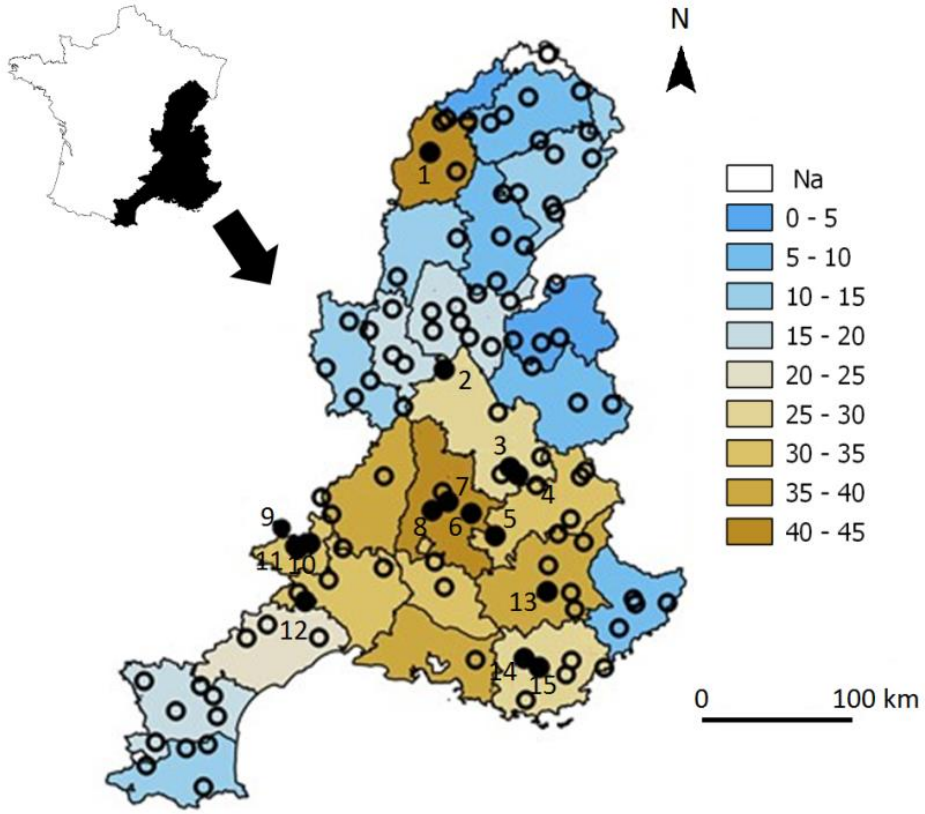

Figure 1: The Rhône-Méditerranée water district, the total number of WR decisions stated by department over the period 2005-2016 and the gauged catchments ○ where WR decisions are simulated (● denotes the subset of the 15 catchments used for evaluation purposes and the figures are the related ranks presented in Table 1).

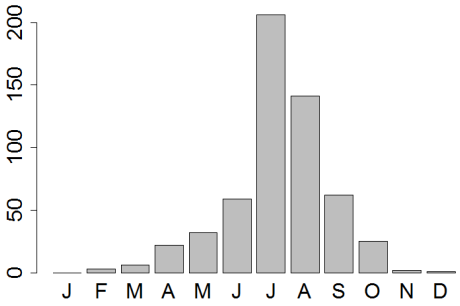

Figure 2: Total number of stated WR decisions over the RM district per month over the period 2005-2016.

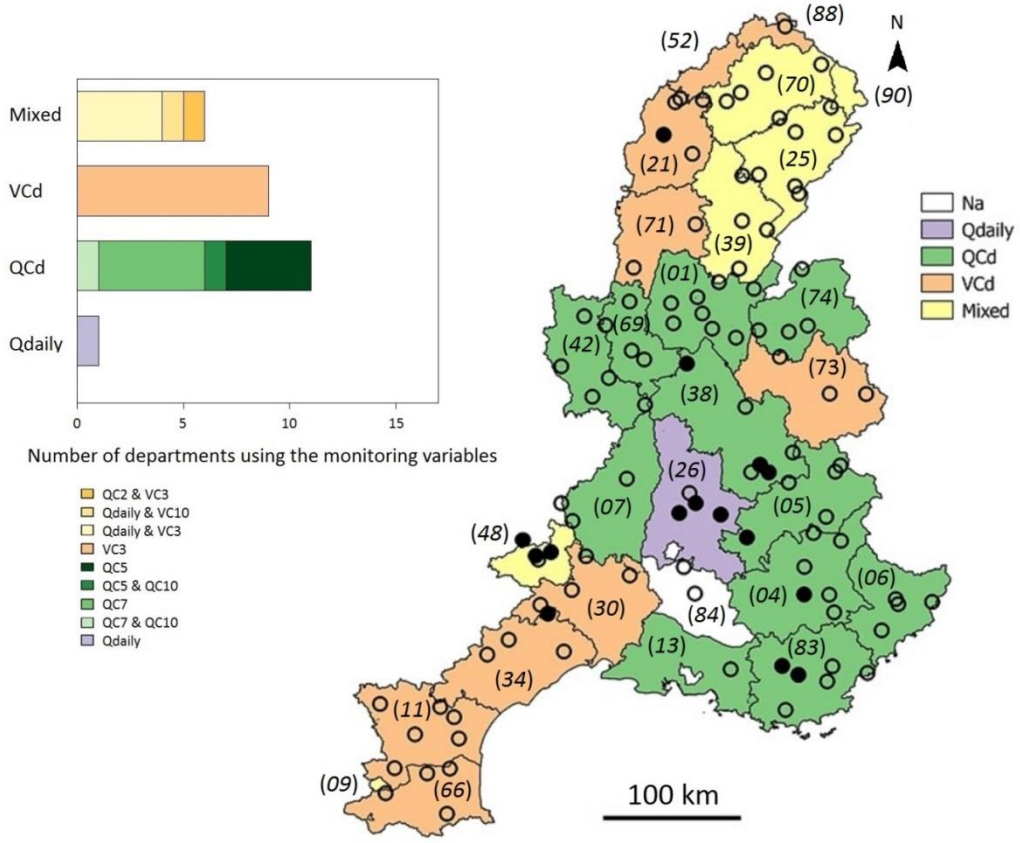

Figure 3: Low-flow monitoring variables used in the current drought management plans. *Qdaily* denotes daily streamflow, *QCd* the *d*-day maximum discharge; *VCd* the *d*-day mean discharge and *Mixed* refers to combinations of the aforementioned variables. Department codes are given into brackets.

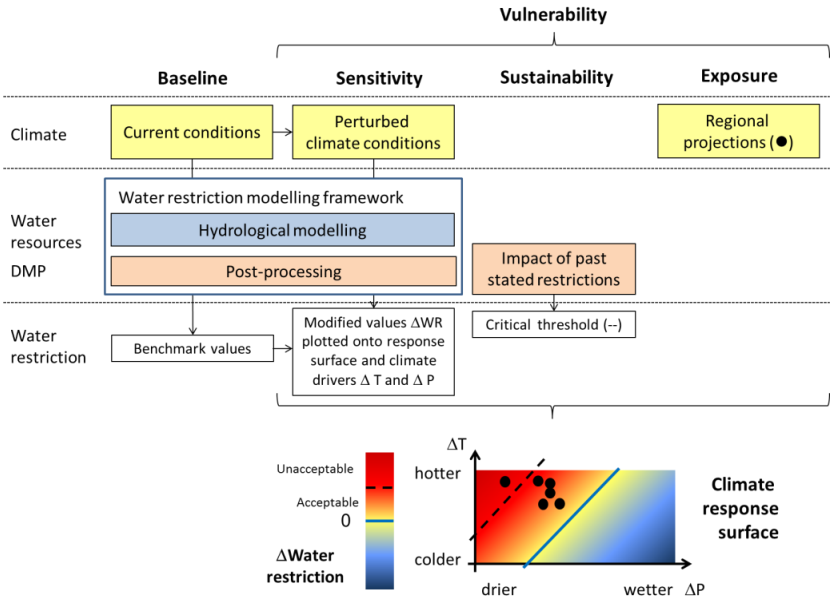

963

964 **Figure 4: Schematic framework of the developed approach to assess the vulnerability of the DMPs under climate**
965 **change.**

966

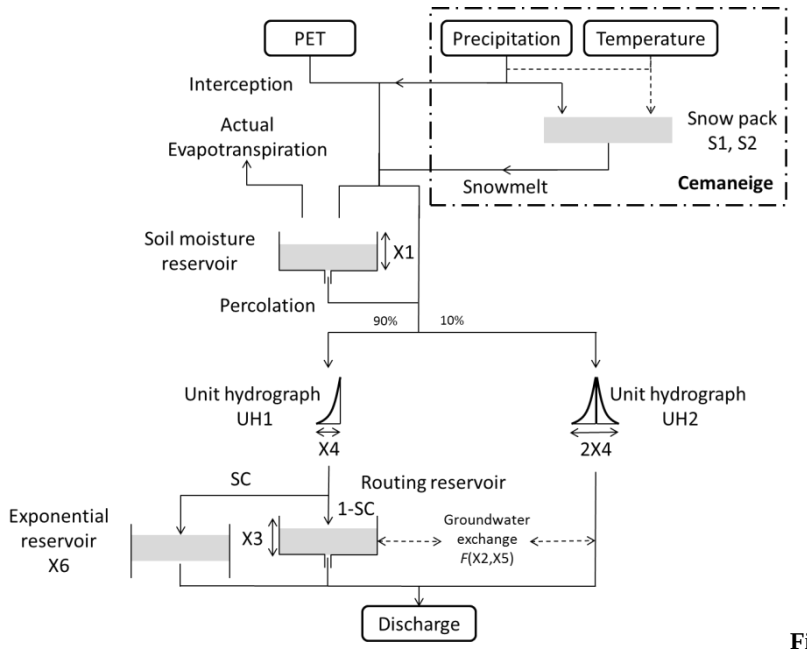

967 **Figure 5: Schematic of the rainfall-**
968 **runoff Model GR6J combined with the CemaNeige snowmelt runoff component (after Pushpalatha *et al.* 2011).**

969

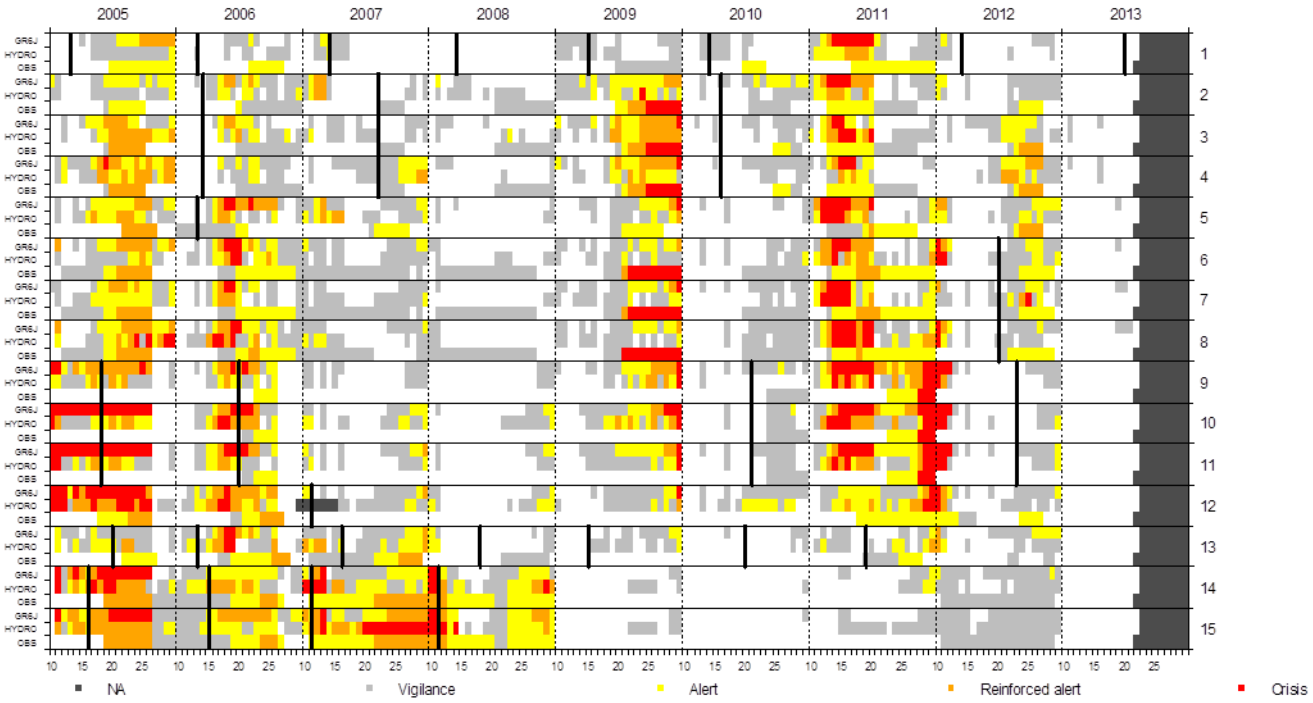

970

971 **Figure 6: Observed and simulated water restriction levels considering the two sources of discharge data GR6J and**
972 **HYDRO for each of the 15 evaluation catchments (Table 1). The x-abscissa is divided into ten-day periods for each**
973 **year spanning the period April-to-October. Black segments identify updated DMPs.**

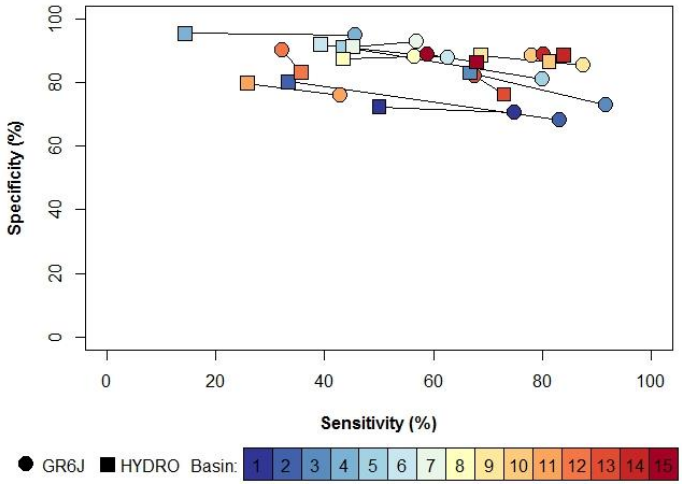

974

975 **Figure 7: Skill scores obtained for the WR level model over the period 2005-2013. Each segment is related to one of**
976 **the 15 catchments listed in Table 2. The endpoints refer to the source of discharge data (GR6J or HYDRO).**

977

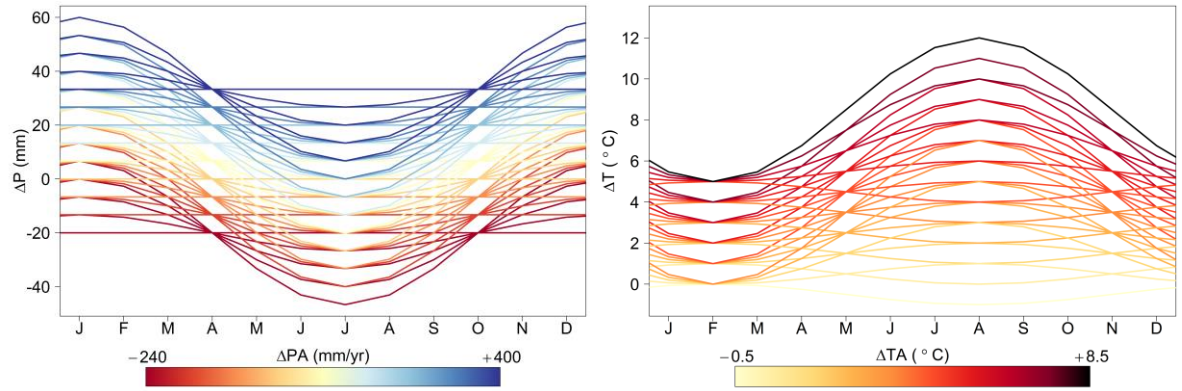

978

979 **Figure 8: Monthly perturbation factors ΔP and ΔT associated with the climate sensitivity domain. The color of the line**
980 **is related to the intensity of the annual change ΔPA and ΔTA.**

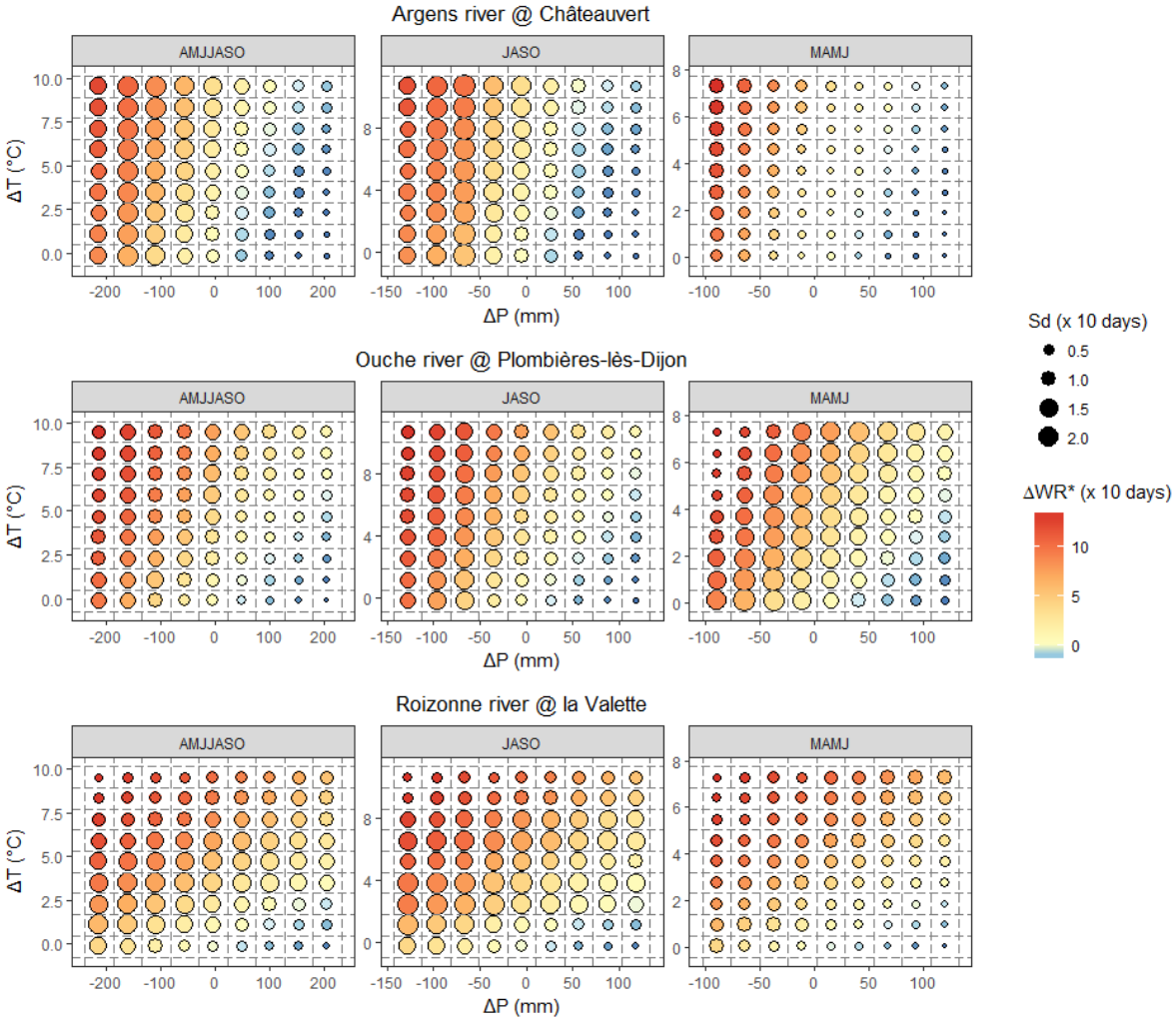

981

982 **Figure 9: Climate response surface of legally-binding water restrictions level anomalies ΔWR* for the Argens, Ouche**
983 **and Roizonne River basins. Each graph is obtained considering changes in mean precipitation ΔP and temperature**
984 **ΔT over a specific period as x- and y-axis.**

985

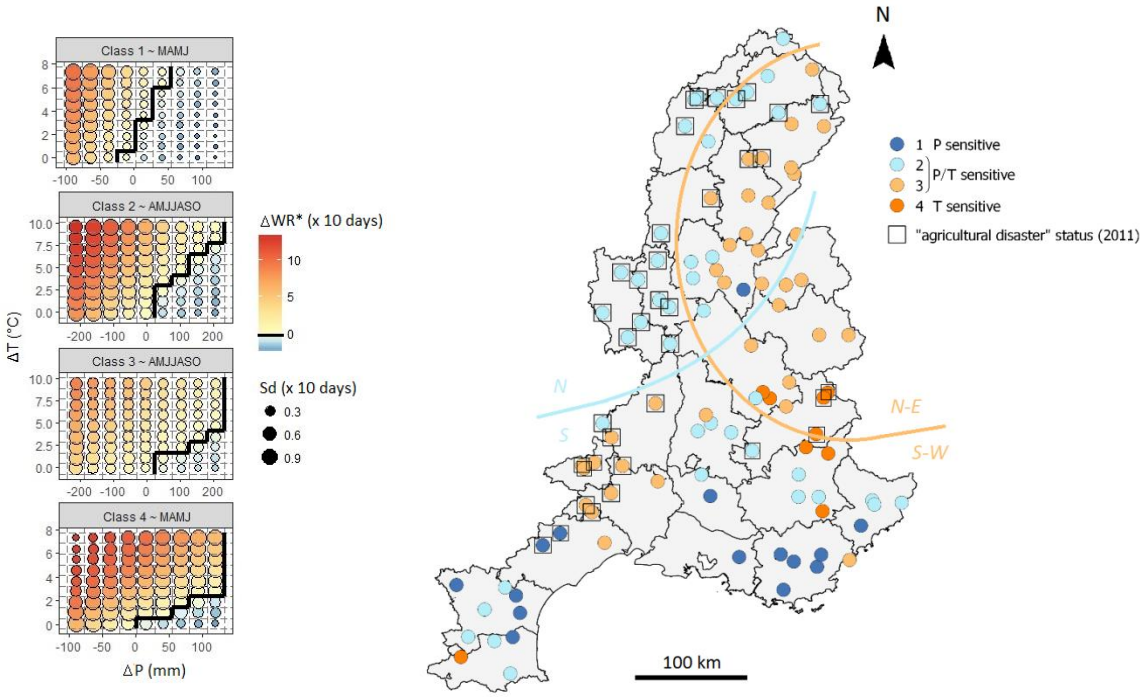

986

987 **Figure 10: Results of the hierarchical cluster analysis applied to the climate response surface WR* level anomalies**
988 **ΔWR***

989

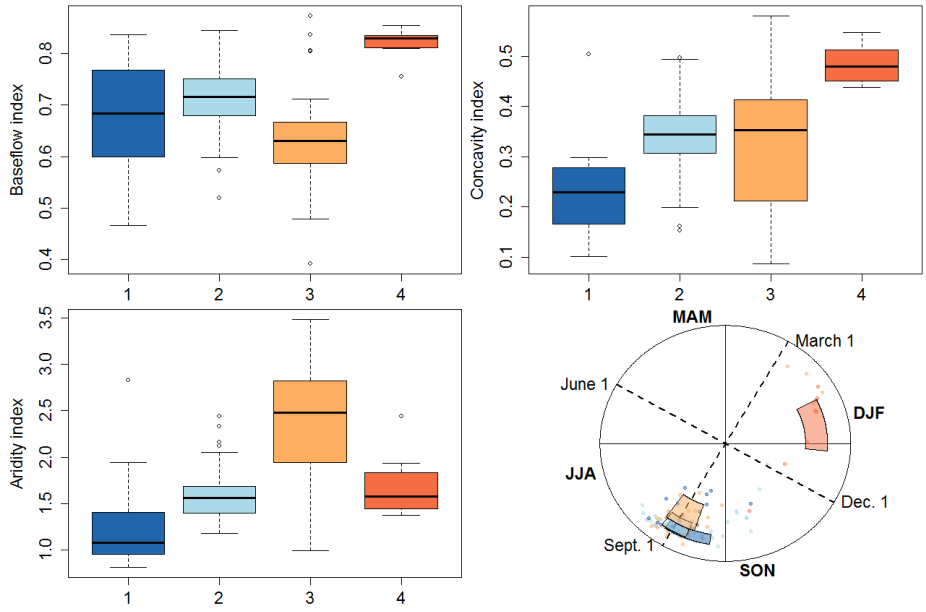

Figure 11: Statistical distribution of the discriminating factors identified by the CART algorithm (top level, top left and bottom left) and the mean timing θ of daily discharge below $Q95$ and its dispersion r (bottom right). The boxplots are defined by the first quartile, the median and the third quartile. The whiskers extend to 1.5 of the interquartile range; open circles indicate outliers. The color is associated to the membership to one class and the name of the class is given along the x-axis. The colored areas in the lower right figure are defined by the first quartile and the third quartile of r and θ. Each dot is related to one gauged basin. The doted lines indicate the start of four meteorological seasons.

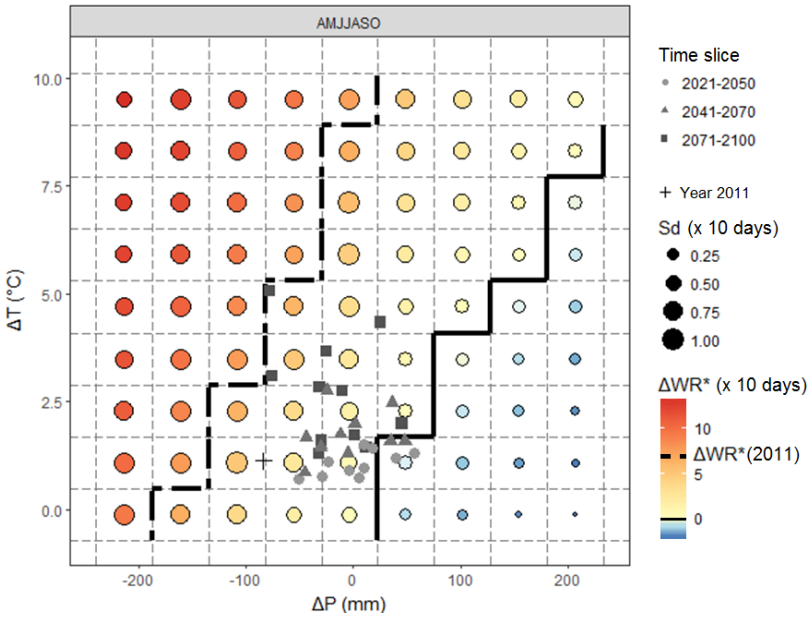

Figure 12: Climate response surface of legally-binding water restrictions level anomalies ΔWR* for the Ouche River basin including both exposure and performance characterizations.

1002

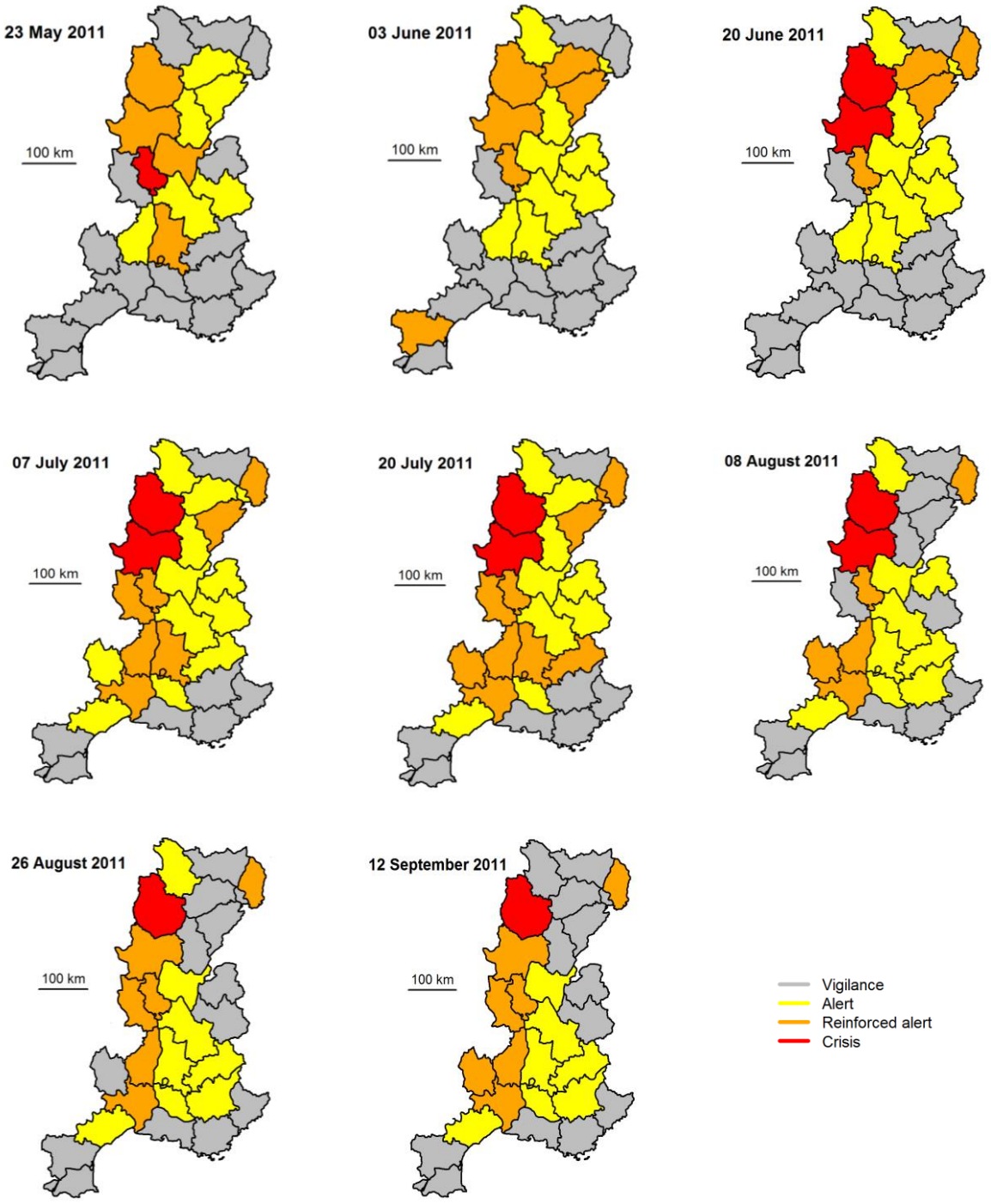

1003 **Figure 13: Most severe water restriction level adopted at the department-level scale for several dates between May**
1004 **and September 2011 (Source: French ministry of Ecology)**

1005

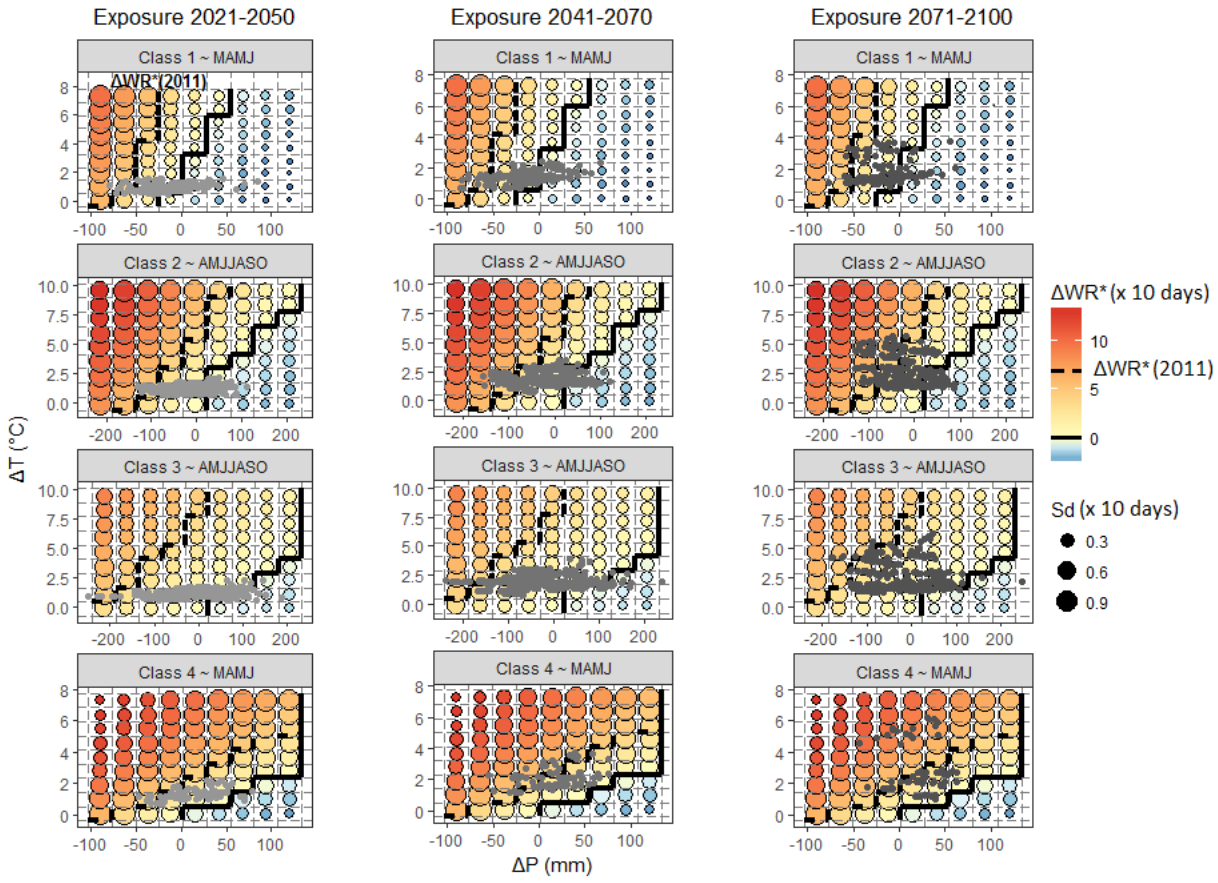

Figure 14: Representative climate response surfaces for each class including both exposure and performance characterizations.

Appendix A: Classification of river flow regime for France

Sauquet *et al.* (2008) have defined a classification based on the mean monthly runoff pattern (Fig. A1) and a map has been published showing the assignment to one class along the main river network. The twelve dimensionless coefficients *CM* are the twelve values of mean monthly runoff (mm) divided by the mean annual runoff).

Groups 1 to 6 are pluvial river flow regimes. The six groups mainly differ by the contrast between the maximum and the minimum of the monthly discharges. Nearly uniform flows through most of the year (Group 1) are found where large aquifers moderate flows whereas Group 6 is characterized by very low flow in summer, reflecting the lack of deep groundwater storages in the catchment. Group 7 is representative of Mediterranean river flow regimes where small rivers basins experience hot and dry summers and intense rainy events in autumn. Their runoff pattern therefore exhibits severe low flow in summer and high flow in November. In mountainous areas, uppermost basins display snowmelt-fed regimes (Groups 10, 11 and 12). The lower the outlet is, the lower the contributions of snowmelt to runoff. Groups 8 to 9 are in the transition regime. The seasonal variation of streamflow is affected as much by precipitation timing as by air temperature and topographic influences (on snowpack formation and snowmelt timing). Typically, high flows are observed in spring.

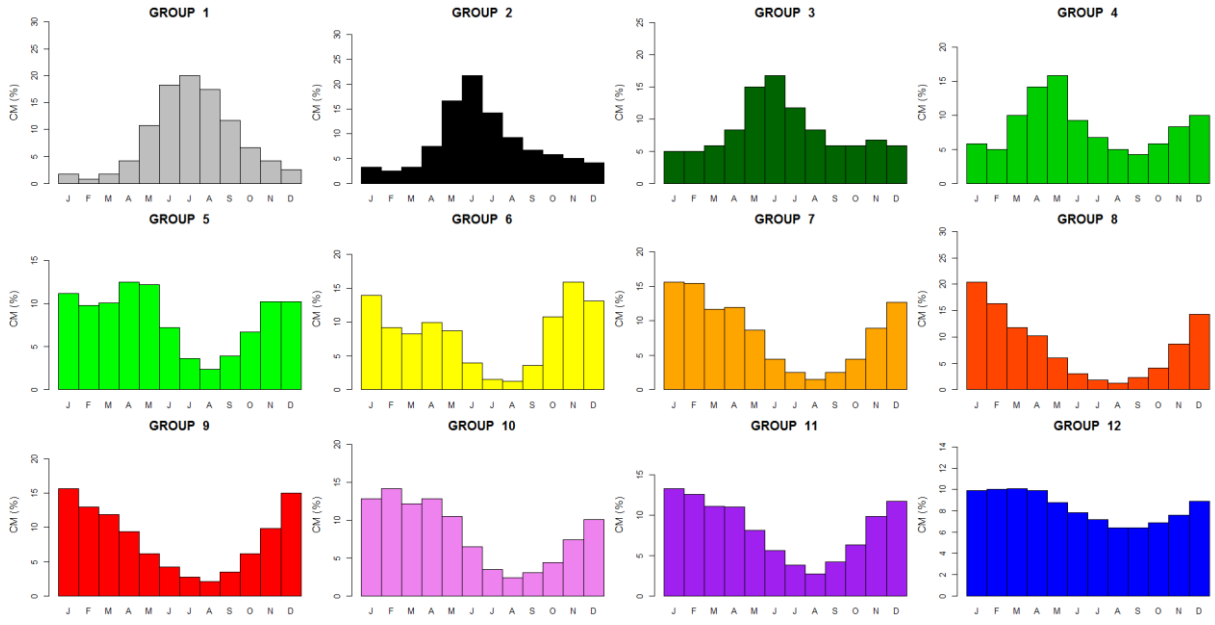

Figure A1 : Reference dimensionless hydrographs representative of the classification of river flow regime for France (after Sauquet *et al.* 2008)